THE CYPRUS INSTITUTE
RESEARCH·TECHNOLOGY·INNOVATION

AN INTRODUCTION TO THE STUDY OF BURNED HUMAN SKELETAL REMAINS

The Cyprus Institute
Science and Technology in Archaeology and Culture Research Center (STARC)

Guide No. 4

Author
Efthymia Nikita

Reviewers:
Colleen Cheverko, Edward Via College of Osteopathic Medicine • Nicholas Herrmann, Texas State University • Simone Lemmers, The Cyprus Institute • Kathryn Marklein, University of Louisville • Ioanna Moutafi, The Malcolm H. Wiener Laboratory for Archaeological Science, American School of Classical Studies at Athens

AN INTRODUCTION TO THE STUDY OF BURNED HUMAN SKELETAL REMAINS

The Cyprus Institute

Science and Technology in Archaeology and Culture Research Center (STARC)

Guide No. 4

Author:
Efthymia Nikita

Reviewers:
Colleen Cheverko, Edward Via College of Osteopathic Medicine • Nicholas Herrmann, Texas State University • Simone Lemmers, The Cyprus Institute • Kathryn Marklein, University of Louisville • Ioanna Moutafi, The Malcolm H. Wiener Laboratory for Archaeological Science, American School of Classical Studies at Athens

Nicosia 2021 (Version 1.0)

CONTENTS

PREFACE

This document is the fourth in a series of guides aimed at promoting best practice in different aspects of archaeological science, produced by members of the Science and Technology in Archaeology and Culture Research Center (STARC) of The Cyprus Institute. The current document was largely developed in the context of two projects: *People in Motion* and *Promised*. The implementation of *People in Motion* involved the laboratory study of a large commingled and partially burned skeletal assemblage from Byzantine Amathus, Cyprus, which came to light in the context of excavations led by the Cypriot Department of Antiquities. Osteological work on this assemblage was co-funded by the European Regional Development Fund and the Republic of Cyprus through the Research and Innovation Foundation (EXCELLENCE/1216/0023). In addition, *Promised* aims at promoting archaeological sciences in the Eastern Mediterranean, with funding from the European Union's Horizon 2020 research and innovation programme under grant agreement No 811068.

The study of burned skeletal remains is particularly challenging due to the extensive alteration of the bones, manifesting as warping, discoloration, shrinkage, and fracturing. These macroscopic changes express underlying structural and chemical alterations. As a result, the application of traditional osteological methods (morphological, metric, chemical, molecular, histological and others) is largely inhibited or should be extremely cautious. Nonetheless, the study of burned skeletal assemblages can offer unique insights to funerary practices and technologies, as well as the manipulation of dead bodies. In line with the above, the aim of this guide is to cover various aspects of the study of burned skeletal assemblages. It should be seen as a supplement to the '*Basic guidelines for the excavation and study of human skeletal remains;* STARC Guide no. 1' and the '*Excavation and study of commingled human skeletal remains;* STARC Guide no. 2'. The current guide is meant to serve only as a general outline and the described field and lab-based methods should be modified depending on the context and characteristics of each assemblage under study.

A number of excellent volumes have been published in the past years, compiling experimental and case studies on the retrieval and examination of burned skeletal remains in archaeological and forensic contexts (Fairgrieve 2008; Schmidt and Symes 2015; Symes et al. 2012; Thompson 2015). Much of the information presented here has been drawn from these resources, as well as from other publications and the author's professional experience. References are given throughout the current document but the aim is by no means to provide an exhaustive account of the literature.

This document is an open resource and it is anticipated to be updated at regular intervals. I would greatly appreciate any feedback and recommendations for future improvement.*

Efthymia Nikita

*For feedback/recommendations, please contact me at e.nikita@cyi.ac.cy

INTRODUCTION

Cremation has been a diachronic practice in many different cultures since prehistory, while bodies may also be exposed to (lower) degrees of heat during mortuary practices such as cleansing fires. Besides funerary practices, a human body may be exposed to fire as a result of different events, such as car or aircraft accidents, bombings, natural disasters, homicides and suicides. In forensic contexts fire can also be used to destroy evidence and hinder the identification of the deceased. For these reasons, any anthropologist working in circumstances where burned skeletal remains may be encountered should possess a general understanding of the physical and biochemical alterations bone and teeth undergo when exposed to varying degrees of heat. The study of burned human remains poses special challenges compared to the anthropological study of non-thermally altered bones as exposure to heat produces macroscopic color changes, shrinkage, fragmentation, and warping, as well as microscopic structural and chemical changes to bones. To ensure that these alterations are precisely analysed and interpreted in their respective forensic or bioarchaeological context, in turn, requires a specific approach in the field and in the laboratory.

Fire Dynamics

Fire is an oxidation reaction that generates heat and light. There are three requirements in order to make a fire (the so-called 'fire triangle'): heat, oxygen, and fuel (DeHaan 2002, 2015). Heat involves raising the temperature of an object to the lowest temperature at which it will sustain combustion. The amount of oxygen must be such that can sustain combustion. Finally, the fuel refers to the combustible materials that are present and capable of sustaining the fire. The best 'fuel' in the human body is subcutaneous fat (DeHaan and Nurbakhsh 2001). The available amount and interaction of the parts of the fire triangle will determine the duration and intensity of the fire and, therefore, its impact on a body (Devlin and Herrmann 2013).

BONE RESPONSE TO FIRE

Even when subjected to extreme burning, human bodies cannot be completely destroyed (Bass 1984; Brickley 2007; Eckert et al. 1988; Zana et al. 2017). In general, the effects of fire on human tissue vary based on the proximity of the body to the fire, the temperature reached, and the duration of exposure to the fire (Fairgrieve 2008). It should be remembered that during the thermal exposure of a body, these parameters alter as temperature, heat and ventilation conditions can fluctuate dramatically (DeHaan 2015). In addition, the preincineration condition of bone, that is, the preservation of blood, marrow, moisture, and fat, also influences heat-induced alterations (DeHaan and Nurbakhsh 2001).

Myth busting

'Spontaneous combustion' and the 'exploding skull' are two myths regarding the human body's response to fire. The former implies the near complete cremation of human bone under unexpected circumstances. Experimental studies have shown that while humans do not spontaneously combust, they are particularly combustible under certain circumstances, such as when bones are osteoporotic (Christensen 2002; DeHaan and Nurbakhsh 2001). With regard to the 'exploding skull', contrary to popular opinion (Heglar 1984; Rhine 1998), the cranium does not explode when exposed to prolonged heat. Pope and Smith (2004) found that numerous factors may fracture a burned skull, such as falling debris, the handling of burned remains, the means by which the fire is extinguished, and others, and these external events is what creates the appearance of the exploded skull.

The temperature reached during heat exposure depends on the amount of oxygen available, the size and volume of the body, the clothing and other layers surrounding the body, and others (Binford 1963; Christensen 2002; Symes et al. 2015). Soft tissues surrounding the bones have a protective effect as they limit the transfer of heat and restrict oxygen supply to the skeleton. This protective effect depends upon the thickness of soft tissues, thus bones surrounded by thinner layers of soft tissues will be exposed to higher temperatures and levels of oxygen before bones protected by thicker soft tissue layers, which will take longer to be affected by the fire (Fairgrieve 2008; McKinley 2015).

A typical outcome of heat-induced shrinkage of muscles, tendons and ligaments is the arrangement of the body in the so-called 'pugilistic posture' (Symes et al. 2015; Ubelaker 2009). The 'pugilistic posture' will provide further protection for some anatomical regions, hence the pattern described in the previous paragraph may not be observed (Thompson 2015). Figure 1 presents the pattern of thermal destruction of a skeleton at pugilistic posture, indicating the initial, secondary, and final areas to be affected by burning (from Symes et al. 2015). It must be stressed again that Figure 1 provides only a very general pattern, while in reality the sequence of skeletal fire alteration is affected by many parameters, such as the position of the body on the fire, the pre-burning condition of the body, the size of the individual, prior pathological conditions, and many others (Symes et al. 2012).
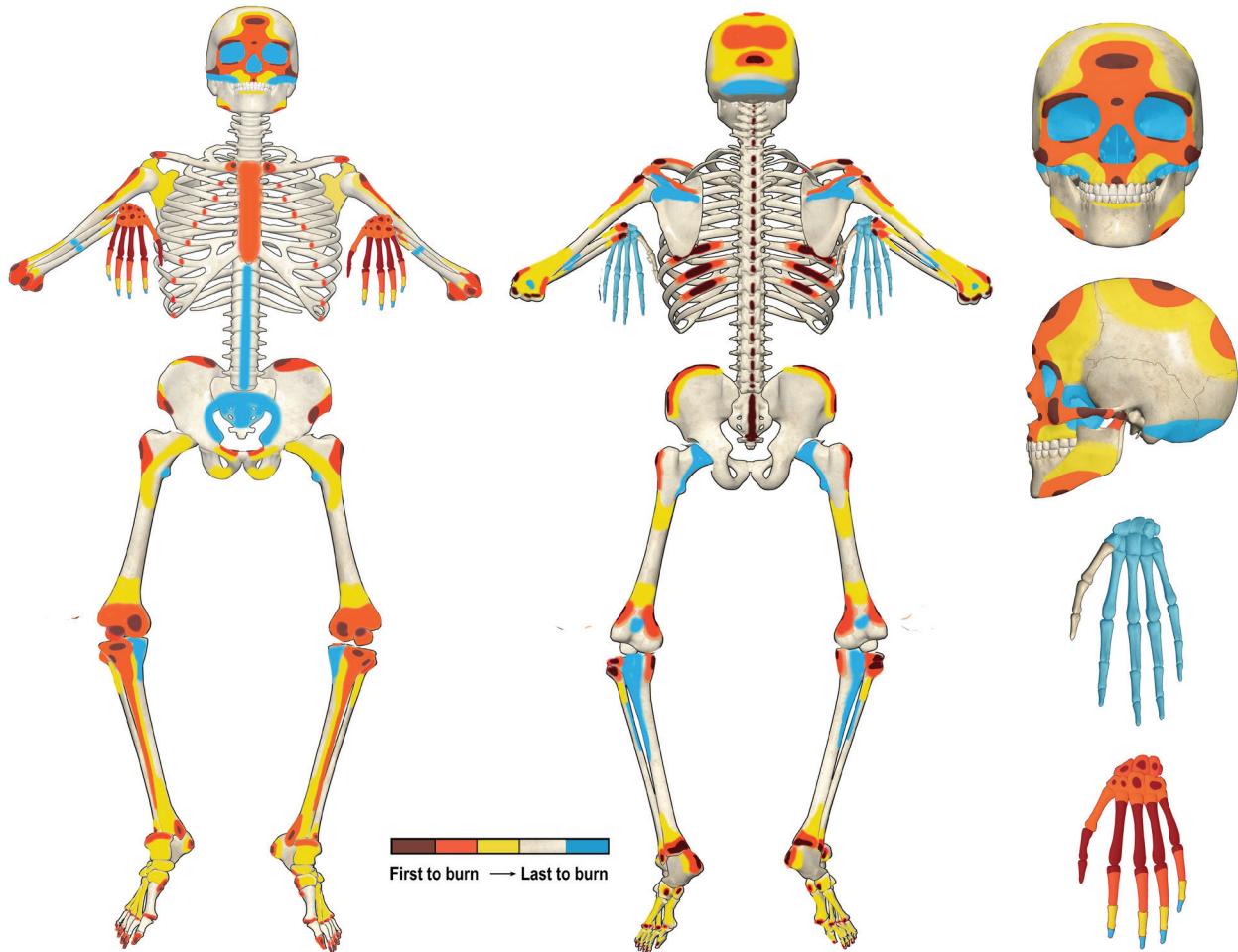
Figure 1. Sequence of skeletal affliction by fire in pugilistic posture (adapted from Symes et al. 2015 Figure 2.7)

A literature review regarding the stages of heat-induced bone transformation has been carried out by Mayne Correia (1997) and reviewed by Thompson (2003, 2004). Although both authors identify the same four stages, they occasionally disagree about the temperature intervals at which each stage corresponds. The first stage, *dehydration*, is characterised by the breakage of the hydroxyl bonds in hydroxyapatite crystals and water loss, leading to subsequent weight reduction and fracturing (Mayne Correia 1997; Thompson 2003). Using scanning electron microscope (SEM) analysis, dehydration is characterized by bubbles in the external lamellae and cracking (Mayne Correia 1997). Both authors agree that dehydration occurs approximately between 100°C and 600°C. The second stage, *decomposition*,

takes place at 500-800°C according to Mayne Correia (1997) and at 300-800°C according to Thompson (2003, 2004). During this stage, organic components decompose and this results in color change, weight loss, reduction in mechanical strength, and changes in porosity. SEM analysis shows an increase in the diameter of the crystals and the lacunae but bone structure is still recognisable (Mayne Correia 1997). In the third stage, *inversion*, there is an increase in crystal size, the carbonates are removed and magnesium is released, causing additional weight loss (Mayne Correia 1997). Under SEM, cracks are wider and the matrix becomes increasingly more homogeneous, while lacunae become less visible. The inversion stage occurs between 700°C and 1100°C according to Mayne Correia (1997) and between 500°C and 1100°C based on Thompson (2004). The last stage, *fusion*, is characterised by the melting and coalescence of the crystal matrix (Thompson 2003). An increase in crystal size can be observed, and considerable bone dimensional reduction and an increase in mechanical strength take place (Thompson 2004). This stage occurs at 1600°C+ according to Mayne Correia (1997) but merely at 700°C+ according to Thompson (2004). Note that these four stages 'in themselves do not explain all of the fundamental causal changes occurring within hard tissues, and to date are entirely theoretical' (Thompson 2004, p. 203).

Carbonization

Organic materials contain high proportions of carbon atoms and experience carbonization when exposed to intense heat. During heating, complex organic molecules break down and elements, such as oxygen and hydrogen, are either freed into the atmosphere or combine with other elements, while structural carbon remains. Since naturally occurring carbon is black in color, carbonized bone is also black (Symes et al. 2015).

Calcination

During calcination, the freed carbon from organic molecules is combined with oxygen and forms carbon dioxide (CO_2) or carbon monoxide (CO). Subsequently, it is released into the atmosphere. The remaining bone is comprised of inorganic components, thus its color is white because this is the natural color of hydroxyapatite (Mayne Correia 1997; Mayne Correia and Beattie 2002; Thompson 2004, 2005). Fracturing, shrinkage, and warping accompany calcination (Schwark et al. 2011; Thompson 2004, 2005).

Commercial cremations versus outdoors pyres

Given the importance of the environment in which fire exposure takes place, it is relevant to outline how modern cremations compare to outdoors pyres. Modern commercial cremations take place in gas-fired ovens, where the main chamber is lined with heat-resistant refractory bricks (Davies and Mates 2005). The body is placed inside a body bag, a cardboard box, or a wooden coffin. The temperature is typically 870°C–980°C and the average duration 2–2.5 hours (Rosen 2004). Afterwards, the burned remains are pulverized to reduce further their volume, leaving little diagnostic bone (Symes et al. 2013). By contrast, in outdoors pyres, which require human intervention and constant heat sources, most of the heat is lost to the atmosphere, a constant external heat source is necessary, and the temperature cannot stay uniform throughout the process. A further complicating factor is the wind, the strength and directionality of which will affect heat distribution and temperature maxima. In addition, the heat is directed to the body only from below, whereas in the cremator heat exposure is multi-directional (McKinley 1994a). Once the main pyre structure burns down, the remains will rest on the hot ash bed, and the cremation may continue for several more hours (McKinley 2006). Weather conditions play an important role in the duration for which the pyre will burn: strong winds will make the pyre burn faster but unevenly, while rain will reduce the pyre temperature or even extinguish it (McKinley 2015). The vegetation surrounding the pyre is also important: dry vegetation will increase fire temperature but reduce its duration due to the fast consumption of the fuel; oily vegetation will take longer to ignite and the pyre duration will be prolonged, while with wet vegetation, a fire may not ignite (Symes et al. 2013).

FIELD PROCEDURES

Burned remains may be found in various contexts: on the ground surface, (partially) buried, inside funerary structures, etc. Any field procedure has to be adjusted to the unique challenges posed by each context of recovery and the associated degree of preservation of the remains, the sample size, and the degree of commingling. In some contexts, a confined excavation will be appropriate, while in others, surface surveying will be a necessary first step to document the spread of the remains.

Burned human remains pose two additional and interconnected challenges compared to unburned remains: fragmentation and identification. Burning can lead to extreme bone fragmentation, which hinders recovery in the field. This extreme fragmentation coupled with the morphological, chemical and structural deformities that characterise burned bone, often renders the differentiation between such bone and other materials difficult (Fairgrieve 2008; Ubelaker 2009).

The steps in the recovery of burned remains are summarised in the box below (see also Nikita et al. 2019). During each of these steps, it is important to describe in detail any features and the stratigraphy, including plan and profile maps, as well as measurements. Any post-depositional disturbance should be recorded in detail as well, while soil samples should be taken and sample locations should be documented. The excavation, documentation and recovery should continue until undisturbed strata are visible (Devlin and Herrmann 2013; Fairgrieve 2008).

Steps in the excavation of burned remains (Naji et al. 2014; Schmidt 2015)

1. Identify the extent of the deposit.

2. Photograph and draw the deposit.

3. If the remains are contained in an urn or other pot, transport the pot to the laboratory so that it is excavated in a controlled environment by an osteoarchaeologist. If the remains are not contained in a pot (or in some structure that may be lifted as a block and transported to the lab), excavate them in the field.

4. Construct a reference grid over the deposit.

5. Document and collect all surface findings (i.e., skeletal elements, artifacts etc.).

6. Using a trowel, paint brushes and wooden tools, excavate the burned remains in layers defined by all the fragments that can be removed without disturbing the underlying level (Fairgrieve 2008).

7. Map large fragments (> 3 cm) individually and group smaller ones (< 3 cm) by grid square.

8. Bag separately the remains of each layer. Make sure to label accordingly fragments found in close proximity so as to facilitate reconstructions and fragment identification later on in the lab.

9. Use paper towels to wrap fragile bones prior to transportation and place them inside paper bags. Avoid plastic bags or metal cans as the former encourage moisture and the latter contribute to further fragmentation.

10. Sieve all soil, ideally using a 3mm screen.

Note that for burned remains found inside urns or other contained structures, the use of virtual approaches, such as computed tomography, has proven particularly useful as a first non-invasive step to assess the context prior to destructive micro-excavation (Higgins et al. 2020).

LABORATORY PROCEDURES

As with field procedures, the particular laboratory procedures employed need to be assemblage-specific. The following sections provide a broad outline.

Cleaning

Bones and teeth should be rinsed with tap water, when not too fragile, and left to dry naturally, avoiding direct sunlight. Dry brushing is preferable when cleaning carbonized bone, as its charcoal-like consistency is more friable than calcined bone. Where bone is well preserved, wet sieving using a 1mm mesh size is ideal. If necessary, a soft toothbrush or a wooden cocktail stick may be used to remove adhering dirt (Fairgrieve 2008; Schmidt et al. 2015).

Sorting and Cataloguing

When sorting bones, as much detail as possible should be used in identifying the anatomical location of each fragment, e.g. 'proximal foot phalanx head and shaft' (McKinley 2017). Particularly useful in this respect is the zonation system for partially preserved remains, which divides each skeletal element in sections/zones (Knüsel and Outram 2004 – see also STARC Guide No. 2). Subsequently, the percentage preservation of each zone may be recorded. If it is not possible to identify their anatomical location, bone fragments should be sorted into broader categories (e.g. cranium, thorax, pectoral girdle, upper limb, pelvic girdle, lower limb, unidentifiable) (Devlin and Herrmann 2015). When bones are too partially preserved, they should be classified into even broader groups, such as 'flat,' 'short,' 'epiphysis,' or 'diaphysis.' Due to the friable nature of burned remains, the number of fragments may increase due to handling; hence, recording weights is important (see section **Weights**) (Fairgrieve 2008). Fragments that are particularly small could be divided into size groups and weighted per group (Naji et al. 2014; Schultz et al. 2015).

The bone inventory as a means of assessing the pre-burning condition of remains

When the representation of anatomical regions is atypical, it is most likely that the cremation involved dry skeletons than fleshed bodies. When fleshed bodies are burned, bone loss may occur during the recollection of the remains from the pyre after cremation and/or during their transportation to the final deposition site. If dry bones are burned, bones may be lost during the abovementioned processes as well as before cremation, when the bones are recovered from their original deposition site (Godinho et al. 2019a). In assessing the pre-burning condition of the skeleton based on the bone/tooth inventory, it is particularly relevant to note the presence of small skeletal elements, such as tooth roots or phalanges, as these are the elements most likely to be left behind when skeletonized remains are transported (Lemmers 2012; Masotti et al. 2020).

Each identifiable bone and tooth fragment and each fragment with length over 2 cm should receive a catalog number. The use of ink on the remains should only be done if the bone is not going to be subjected to chemical tests and if such writing will not impede the visibility of important anatomical traits. Due to the friable nature of burned remains, it is preferable to number the bone containers (e.g. bags) rather than the bones themselves (Fairgrieve 2008; Watson et al. 2015).

Reconstruction

Although often impossible to undertake due to the warping of bone fragments, reconstruction/refitting (the articulation of the broken edges of bone fragments) enhances the morphological and metric study of burned remains and can provide important information regarding the dispersal of fragments from a single element across the deposit (Curtin 2015; Ubelaker 2009). Consolidants should be used in moderation, with preference to water- or alcohol-soluble materials (Schmidt 2015).

Minimum Number of Individuals

Burned remains may represent multiple skeletons because many individuals had been burned together or because the pyre area had been used multiple times and debris from successive cremations got mixed or for other reasons (André et al. 2013). The identification of multiple individuals in the same deposit is based on supernumerary bones or skeletal elements with discordant dimensions, age, sex or systematic disease (Irish et al. 2015; Rubini et al. 1997). Note, however, that bone dimensions should be used cautiously because heat exposure results in shrinkage and warping (see section **Shrinkage and warping**). The best approach is to estimate the Minimum Number of Individuals (MNI) using an anatomical area that is particularly dense and less likely to be affected severely by fire, such as the petrous part of the temporal bone (Fairgrieve 2008). The use of more elaborate methods, such as those for the estimation of the Most Likely Number of Individuals (Adams and Konigsberg 2004) or the Initial Number of Individuals (Nikita and Lahr 2011), is often not practical given the very small burned fragments that comprise the majority of cremated assemblages. In cases of partial cremation, however, such methods may be applied in conjunction to MNI estimates.

DNA analysis may also be adopted to sort skeletal elements per individual (Schultz et al. 2015); however, DNA tends to be destroyed above 600°C and often even below that temperature (Walker et al. 2008). Another means of estimating the number of individuals present in an assemblage is the average weight of skeletal remains. The average weight per adult body in modern crematoria is 1,760.3 g to 3,379 g (Bass and Jantz 2004; May 2011; Van Deest et al. 2011). Any greater mass of burned remains supports strongly the presence of more than one individual. Any smaller mass of remains, however, does not necessarily imply that only one individual is represented in the assemblage; instead it may indicate some selection process. Another limitation of this approach is that cremation weights vary greatly based on an individual's age, sex, pathological status and many other factors (Bass and Jantz 2004), while taphonomic factors may alter considerably the weight of burned bone (Amarante et al. 2019). See also section **Weights**.

Sex assessment

Many authors have argued that techniques used for sexing unburned skeletal remains based on the morphology of the skull and pelvis are applicable to cremated individuals (Geber et al. 2017; Lara et al. 2015; Mayne Correia and Beattie 2002; Rubini et al. 1997; Wahl 2015). Nonetheless, Fairgrieve (2008) highlights a number of limitations in the applicability of these criteria due to shrinkage, warping and heat-induced fractures (see sections **Shrinkage and warping** and **Heat-induced fractures**).

The use of osteometric methods to sex burned human remains has also been suggested. Gejvall (1969) proposed metric standards for sex estimation based on skull thickness, humeral head diameter, and femoral, humeral and radial diaphyseal thickness. Warren and Maples (1997) also used femoral and humeral head measurements of burned human remains and found that femoral head measurements had an average of 44.2 mm for males and 38.2 mm for females, and humeral head measurements had an average of 45.8 mm for males and 38.2 mm for females. Van Vark (1975) and Van Vark et al. (1996) examined the expression of different cranial and post-cranial sexually dimorphic traits on a cremated sample from 19th century Amsterdam. The results were extremely good for the male individuals (92% correct classification) and reasonable for the female individuals (79% correct classification). In addition, Schutkowski (1983) and Schutkowski and Herrmann (1983) obtained correct sex classification in 67.0% - 73.4% of the cases examined using discriminant function analysis on the petrous bone. Similarly, Gonçalves et al. (2013a) achieved successful sex classification scores using humeral, femoral, talar and calcaneal measurements from Portuguese cremated individuals. However, other metric sexing methods, such as the lateral angle of the internal auditory canal, have been found not to provide accurate results with burned human skeletal remains (Gonçalves et al. 2015a; but see Masotti et al. 2019). It must be stressed that metric sex estimation is based on population-specific samples, so the application of such methods should be cautious, whether in burned or unburned remains.

Logistic regression equations for sex estimation (adapted from Tables 6 and 7 in Gonçalves et al. 2013a)*

- -32.753 + 0.891 * Humeral head transverse diameter
- -26.919 + 0.661 * Humeral head vertical diameter
- -49.415 + 0.904 * Humeral epicondylar breadth
- -29.896 + 0.782 * Femoral head transverse diameter
- -30.376 + 0.759 * Femoral head vertical diameter
- -32.849 + 0.683 * Talar maximum length
- -39.628 + 0.549 * Calcaneal maximum length
- -37.626 + 0.825 * Humeral head transverse diameter + 0.177 * Humeral head vertical diameter
- -36.860 + 0.664 * Femoral head transverse diameter + 0.299 * Femoral head vertical diameter

Positive values suggest males, while negative values suggest females

More recently, Cavazzuti et al. (2019) proposed cut-off points for osteometric sexing in archaeological populations (Table 1). To develop their method, the authors used Bronze Age and Iron Age cremated individuals from Italy. An important caveat of their study is that the sex of these individuals was assessed on the basis of 'clearly engendered grave goods', thus it was based on the assumption that gender was highly correlated to sex in these groups.

Gouveia et al. (2017) examined the potential of odontometric sex estimation on experimentally heated teeth and found that this approach has serious limitations, though certain dimensions and combinations of variables (cementum-enamel junction perimeter, combined mesiodistal and buccolingual diameters) may reach correct sex classification that exceeds 80%. In contrast, Godinho et al. (2019b) found that micro-fracturing produces statistically significant expansion of the tooth crown, which impacts odontometric sex estimation. The authors highlighted that the effect of heat-induced size changes may be removed using μCT scanning; however, this is a complex approach and, coupled with the fact that tooth crowns tend to fracture when exposed to high temperatures, renders odontometric sexing impractical.

Finally, studies using the weight of burned remains to discriminate between sexes (Van Deest et al. 2011) should be considered tentative at best (Naji et al. 2014). Although the difference between female and male weights is often statistically significant, the range of variation and the often incomplete state of the skeleton in burned assemblages due to various taphonomic processes additionally to heat exposure, strongly limit sex assessment using cremated weights. In addition, age-related differences also interfere with relevant assessments (Gonçalves 2011). See also section **Weights**.

Table 1. Cut-off points for osteometric sexing based on ancient Italian populations (adapted from Cavazzuti et al. 2019 Tables 3 and 4)*

Skeletal Element	Measurement	Cut-off point (mm)
Mandible	condyle width	15.87
Axis	dens anteroposterior diameter	9.55
Axis	dens transverse diameter	9.10
Humerus	vertical head diameter	37.88
Humerus	trochlea maximum diameter	20.00

Skeletal Element	Measurement	Cut-off point (mm)
Humerus	trochlea minimum diameter	13.28
Humerus	capitulum maximum diameter	16.09
Radius	**head maximum diameter**	18.32
Lunate	maximum width	14.30
Lunate	**maximum length**	13.82
Femur	**vertical head diameter**	39.39
Patella	maximum height	35.68
Patella	**maximum width**	36.61
Patella	maximum thickness	16.10
Talus	maximum length	46.87
Talus	head-neck length	16.51
Talus	**trochlea length**	28.92
Talus	trochlea width	27.52
Navicular	maximum lenght	13.46
First metatarsal	dorsoplantar width of the head	16.17
First metatarsal	**mediolateral width of the head**	17.02

Key: Values greater than the cut-off point suggest males, while smaller values suggest females; Measurements in bold are those that showed accuracy equal to or higher than 80% in the cross-validation analysis.

Age-at-death estimation

To determine age-at-death in burned remains, scholars use the same osteological methods as for unburned skeletal remains (Geber et al. 2017; Irish et al. 2015; Lara et al. 2015; Mayne Correia 1997; Mayne Correia and Beattie 2002; Rubini et al. 1997), unless the remains are so partially preserved that it is possible to only distinguish between 'nonadult' (<18 years) and 'adult' (>18 years) (Curtin 2015; McKinley 2017). Even in cases where traditional ageing methods can be applied, one needs to bear in mind the impact of heat-induced alterations (Table 2).

Special reference should be made to metric and histological methods and their applicability to ageing burned remains. When using metrics to age burned nonadults, it should be remembered that fire exposure results in a reduction in bone dimensions. Fazekas and Kósa (1978) make reference to the study by Petersohn and Köhler (1965) where percent shrinkage was examined on fetal bones as these passed through the fresh, carbonized and calcined states. Huxley and Kósa (1999) reevaluated Petersohn and Köhler's (1965) data and noted that shrinkage from carbonization and calcination exhibits great variation depending on the lunar month and the skeletal element. Table 3 is a compilation by Huxley (1998) of Petersohn and Köhler's (1965) data showing the differences in the average percent shrinkage of different skeletal elements per lunar month.

Table 2. Influence of heat-induced changes on age-at-death estimation methods (adapted from Fairgrieve 2008 Table 5.6)

Ageing method	Heat-induced alteration
Primary ossification centers	Destruction, especially of infant wrist and cranial bone cartilaginous ossification centers
Tooth formation & eruption	Desiccation of tooth crown and roots
Epiphyseal fusion	Fracturing of epiphysis and fusion sites, destruction of growth plate
Pubic symphysis morphology	Fracturing, warping, bone surface deformity
Auricular surface morphology	Fracturing, warping, bone surface deformity
Sternal rib ends morphology	Fracturing, destruction
Cranial suture closure	Fracturing, delamination

Table 3. Comparison of shrinkage rates (%) by skeletal element for fetuses between 4–10 lunar months (LM) and newborns (drawn from Huxley 1998 Table 7; reprinted by Fairgrieve 2008 Table 5.5)

	4LM	5LM	6LM	7LM	8LM	9LM	10LM	Newborn
Humerus	9.13	5.39	3.37	2.24	1.45	1.68	1.75	2.03
Radius	9.73	5.79	4.30	2.24	2.41	1.90	1.70	0.39
Ulna	9.23	5.65	3.46	2.25	2.21	1.82	3.09	1.06
Femur	13.85	4.59	3.56	2.46	2.28	1.67	1.72	1.48
Tibia	12.35	5.82	3.44	2.51	2.93	1.94	1.69	1.19
Fibula	6.27	7.18	2.77	2.07	1.82	1.59	1.46	1.52

With regard to histological methods, Bradtmiller and Buikstra (1984) found that bone burned at 600°C could provide accurate microscopic age estimates. More recently, Absolonova et al. (2013) tested the effect of higher temperatures of exposure (700°C, 800°C, 1000°C) on bone microstructure and found a decrease in the dimensions of the microstructures and an increase in their number per mm^2 induced by age, but also by burning within the same age group. The authors highlighted that burning-induced microstructural changes are similar to age-related changes, which reduces the applicability of age-at-death estimation equations, especially for remains burned at temperatures over 800°C. For this reason, the authors developed new regression equations for unburned bones, bones burned at 700°C, and at 800°C (Tables 4-5).

Table 4. Histomorphometric variables used in age-at-death estimation equations (adapted from Absolonova et al. 2013 Table 2)

Variable	Abbreviation and Unit
Number of intact osteons per mm^2	POC_OST; #/mm^2*
Osteon circumference	OBV_O; µm
Maximal osteon axis	MAX_O; µm
Haversian canal feret diameter	F_PR_K; µm
Haversian canal shape factor	SFAC_KAN
Number of non-Haversian canals per mm^2	P_NON_H; #/mm^2
Percentage of total internal circumferential lamellae area	PR_LAM; %

*#/mm^2 is the number of microstructures per mm^2 of the compact bone area

Table 5. Age-at-death prediction equations for pooled sexes (adapted from Absolonova et al. 2013 Tables 5-7)

Fire temperature	Equation	r	SEE
Unburned	Y = 163.0256 - 0.1449(OBV_O) - 0.4786(PR_LAM) - 6.7111(P_NON_H)	0.761	13.924
700°C	Y = -59.8169 - 0.2822(MAX_O) + 222.6290(SFAC_KAN)	0. 673	16.248
800°C	Y = 100.5203 - 0.353(MAX_O) + 0.4769(F_PR_K) + 0.4136(POC_OST)	0.578	14.903

The accuracy of histological methods

It must be noted that even in unburned remains, the use of histological age-at-death estimation should be cautious with many scholars pointing out that histological methods should merely be used as a rough age-at-death indication (e.g. Chan et al. 2007; García-Donas et al. 2016; Lagacé et al. 2019; Paine and Brenton 2006).

Heat exposure also affects the identification of dental age-at-death indicators, such as the apposition of secondary dentin, dentinal sclerosis and cementum incremental lines (Gocha and Schutkowski 2013; Naji et al. 2014).

Stature estimation

The application of methods of stature estimation based on fragmentary bones has been attempted by various researchers studying burned remains (Lisowski 1968; Malinowski and Porawski 1969; Piontek 1975; Rösing 1977). However, these studies recognize that the error rates for such estimates are large due to bone shrinkage (Holland 1992; Mayne Correia 1997). Fairgrieve (2008) suggests the adoption of a correction factor to account for bone shrinkage when applying one of the various methods available for stature estimation. However, the degree of bone shrinkage is usually unknown. Thus, stature estimates should only be attempted for skeletal elements that appear to have had limited heat exposure.

Pathology

Shrinkage, warping and fragmentation obscure pathological assessments. However, certain types of pathology, such as degenerative disease and porotic hyperostosis, can be reliably identified even on small burned fragments (Reinhard 1994). A key issue with the study of burned remains is the identification of trauma, as detailed below.

Trauma

Even though in burned remains, sharp-force, blunt-force and ballistic trauma may be difficult to discern, experimental studies indicate that diagnostic evidence often survives heat exposure. Herrmann and Bennett (1999) showed that sharp-force trauma can be recognized after incineration (see also Figure 2), but this was not the case for ballistic trauma due to the extensive fragmentation it generated prior to burning. Blunt-force trauma could be identified in most cases but required the reconstruction of the skeletal elements prior to any assessment. The authors also noted that larger bone fragments were associated with traumatic fracturing whereas smaller fragments and perpendicular fracture angles with heat-induced fracturing. Regarding longitudinal fractures, smooth surfaces were most frequently associated with traumatically induced fractures. Looking into different types of sharp-force trauma, de Gruchy and Rogers (2002) found that chop marks could be identified on burned bone, whereas hacking made the bone more prone to heat-induced fragmentation. In the same direction, Kooi and Fairgrieve (2013) concluded that temperature, fuel, oxygen availability and general burning environment affect cut mark preservation; however, they also stressed the shielding effect that soft tissue has in low temperatures. In contrast, Waltenberger and Schutkowski (2017) concluded that despite heat-induced alterations, cut marks can be identified on burned bones, as the variables principally affected are the slope height and floor angle of the cut, whereas the depth, width, slope, opening angles and floor radius are not significantly influenced by fire. This is in agreement with Tutor et al. (2021), who examined experimentally inflicted sharp-force trauma by means of a machete and a serrated knife on pre-burned bones and were able to distinguish cut marks from heat-induced alterations, though some heat-induced fractures (e.g. step and transverse fractures) can be mistaken with trauma. In contrast, cut marks inflicted again with a machete and a serrated knife but this time on bones that were subsequently burned, were largely eliminated after heat exposure (Tutor et al. 2020). With regard to saw marks, Marciniak (2009) showed that heat exposure affected the identifiability of saw mark striae, but the marks left by most types of handsaws and power saws could be discriminated, and Robbins et al. (2015) found that the saw striae characteristics identified in burned samples using SEM and stereomicroscopy were in agreement to each other. Collini et al. (2015) analysed blunt-force trauma, drill injuries and gunshot wounds in experimentally charred bones. Morphological trauma features were overall preserved after heat exposure, but depressed fractures increased in dimensions, drilled injuries shrunk, and the number of fractures increased in samples with gunshot wounds. Finally, Pope and Smith (2004) examined cranial trauma and found that identification of ballistic, blunt-force, and sharp-force wounds is possible, as detailed in Table 6; in contrast, Franceschetti et al. (2021) concluded that peri-mortem cranial fractures are rarely possible to identify post-cremation.

Figure 2. Pre-burning sharp-force trauma – note sharp margins compared to irregular margins of fire-induced fractures (adapted from Devlin and Herrmann 2013 Figure 16.13)

Table 6. Summary of heat effects on cranial trauma (adapted from Pope and Smith 2004 Table 2)

Type of trauma	Heat-related bone changes	Trauma signatures in burned crania
ballistic	• Focal retraction and shrinkage of wounds • Advanced destruction of exposed injuries • Accelerated bone color changes in open injuries	• Internal or external beveling • Secondary radiating or concentric fractures • Juxtaposition of color in adjacent fragments • Radiating fractures into green bone • Deformed, ragged, or eroded fracture margins
blunt-force	• Focal retraction and shrinkage of impact sites • Advanced destruction of exposed injuries • Accelerated bone color changes in open injuries	• Impact sites exhibiting tool marks or inwardly crushed bone • Secondary radiating or concentric fractures • Juxtaposition of color in adjacent fragments • Radiating fractures into green bone • Deformed, ragged, or eroded fracture margins • Depression, inward crushing, and tool marks
sharp-force	• Focal retraction and shrinkage of incisions • Advanced destruction of exposed injuries • Accelerated bone color changes in open injuries	• Linear incisions, depressions, cuts, chops, saw marks, punctures, stabs, hacks, drill marks, and other tool marks
control	• Bone color changes according to degree of heat exposure	• Delamination, fragmentation, embrittlement, and color changes • "Exploded appearance"

Heat-induced fractures

Heat-altered bone gradually loses its water and organic components, and becomes susceptible to compressive and tensile forces, resulting in heat-induced fractures (Mayne 1990). The degree of bone fragmentation depends upon three factors: fire temperature, fire duration, and existence of mechanical trauma. In temperatures under 700°C, there is little fragmentation, except in the long bone epiphyses (Bohnert et al. 1998; Pope and Smith 2004), while at temperatures over 700-800°C, bones become more fragile (Marella et al. 2012; Pope and Smith 2004). Even though fire duration is important, greater bone fragmentation does not necessarily imply a longer duration of fire exposure. DeHaan (2012) experimented with a seven-hour fire and found that the head and upper limbs were left largely intact. Similarly, Spitz (1993) found identifiable bone fragments even after one or two days of fire exposure.

Symes and colleagues (2013, 2015) discuss at length the biomechanics of burned bone and propose seven classes of heat-induced fractures (Figures 3-4):

1. Longitudinal: Longitudinal fractures are the most common burn fractures in long bones. They are usually parallel to the osteon canals, although they may also exhibit a somewhat helical direction down the long bone axis. They may penetrate the marrow cavity.

2. Step: Step fractures extend transversely from one longitudinal fracture to another.

3. Transverse (or straight transverse): Transverse fractures are very common; they are perpendicular to the long bone axis. They tend to penetrate the medullary cavity and may completely transect the bone. They are very similar to or comprise step fractures.

4. Patina: Patina fractures are superficial and appear as a mesh of uniform small cracks. They are found mostly on the flat surfaces of postcranial bones, the epiphyses and the cranial bones.

5. Splintering and Delamination: These fractures are expressed as a separation of cortical from trabecular bone, and they are mostly found in the cranial bones, the epiphyses and the costochondral rib ends.

6. Burn line fractures: These fractures separate the burned from the unburned bone surface.

7. Curved transverse (curvilinear): These fractures circumscribe the long bone shaft. They may extend from longitudinal fractures or show an oblique orientation. A less common type manifests as 'concentric rings.'
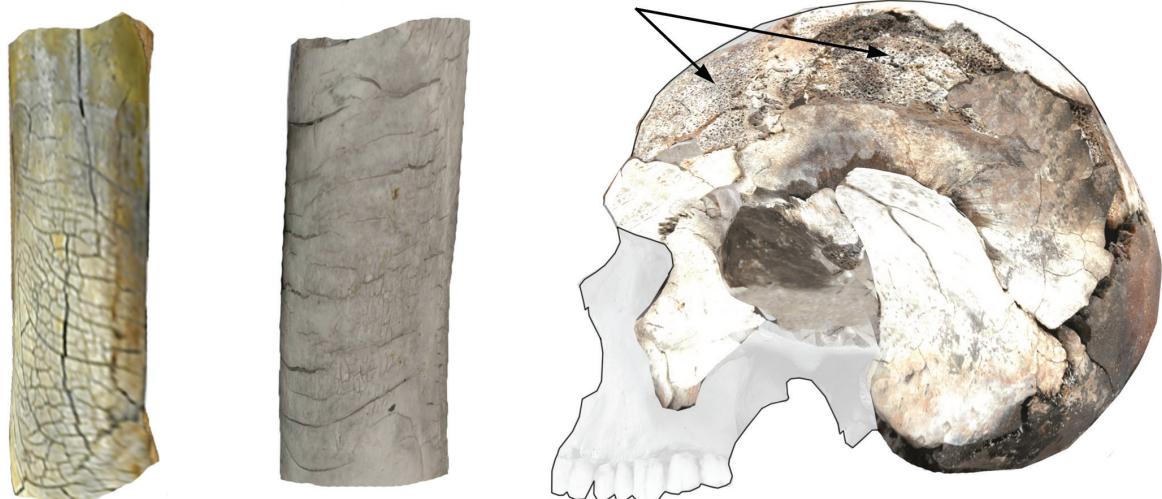

Figure 3. Patina fracture with transverse, longitudinal and curved transverse fractures (left) (adapted from Symes et al. 2013 Figure 14.16), transverse fractures (middle) and delamination (right) (adapted from Devlin and Herrmann 2013 Figures 16.6 and 16.8)

Figure 4. Curved transverse fractures at distal femur (left) (adapted from Symes et al. 2013 Figure 14.10) and unidentified long bone (right) (adapted from Gonçalves et al. 2011 Figure 2)

Recording fragmentation

The maximum length of each bone fragment should be recorded using a sliding calliper (Bontrager and Nawrocki 2015; Watson et al. 2015). Subsequently, the percentage of bone fragments smaller than 1 or 2 cm indicates the intensity of fragmentation (Curtin 2015; Lyman 1994). For example, Minozzi (2015) sorted the degree of bone fragmentation into three categories: *high* if more than 50% of the remains were smaller than 2×2cm, *medium* if more than 50% of the remains were larger than 2×2cm, and *low* if more than 50% of the remains were larger than 5×2cm. Alternatively, the relative fragmentation of bone can be estimated by the ratio of the number of fragments recovered to the minimum number of elements. The higher this value, the more fragmented the bones (Costamagno et al. 2005; Lyman 1994).

For particularly fragmented remains, the Fragmentation Index proposed by Harvig and Lynnerup (2013) may be used. This is the ratio of cremation weight (in grams) to cremation volume (in millilitres). A Fragmentation Index below 1 represents limited fragmentation, whereas a Fragmentation Index above 1 represents substantial fragmentation.

Shrinkage and warping

Heat-induced dimensional change (bone shrinkage) has been noted in a number of early experimental studies (Dokládal 1971; Malinowski and Porawski 1969; Piontek 1975). Among the most systematic early studies were those by Herrmann (1976, 1977), who heated cortical bone at 150°C to 1200°C and identified three phases of shrinkage:

1. 150-300°C, resulting in 1-2% shrinkage
2. 750-800°C, also resulting in 1-2% shrinkage
3. 1000-1200°C, resulting in 14-18% shrinkage

More recently, Byers (2005) confirmed the above results as he found minimal to 2% bone shrinkage at temperatures up to 700°C, 1-2% shrinkage at temperatures of 700-800°C, and 10-15% shrinkage at temperatures over 800°C. Subsequent studies using different skeletal elements and temperatures have concluded that the expected shrinkage

in cremated bone is limited up to temperatures of 800°C; however, above this temperature, shrinkage should be taken into consideration when applying morphological and metric skeletal methods (Bradtmiller and Buikstra 1984; Buikstra and Swegle 1989; Grupe and Herrmann 1983; Holland 1989; Hummel and Schutkowski 1986; Nelson 1992; van Vark 1970).

Thompson (2005) found a wide range of dimensional changes on bones burned at different temperatures (500°, 700°, 900°) for different lengths of time (15', 45') and measured at different points after removal from the furnace (5', 15', 25'): -4.5% to 13.0% dimensional change for bones burned up to 500°C, -1.7 to 19.3% for bones burned up to 700°C, and -3.9% to 37.7% for bones burned at 900°C. Thompson's (2005) results highlighted that the duration of fire exposure is also important. Gonçalves' (2011) experimental work supported this statement but stressed that the relationship between shrinkage and exposure duration is not linear.

As for the relationship between bone mineral content and shrinkage, Herrmann (1976, 1977) found higher percent shrinkage for males in comparison to females, which he associated to higher percentages of bone mineral in the former. In contrast, Huxley and Kósa (1999) found decreased shrinkage of heat-exposed bones with increasing age in foetuses; therefore, a negative association between shrinkage and bone mineralization (Guo 2001). In addition, mean shrinkage rates in foetuses have been found by many authors to exceed those seen in adults due to the relatively higher proportion of collagenous distribution within developing nonadult bones (Bradtmiller and Buikstra 1984; Harsányi 1993; Herrmann 1977; Holland 1989; Müller et al. 1952). These findings support that skeletal elements become less susceptible to heat-induced shrinkage as bone mineralization progresses.

Another important factor determining the degree of shrinkage is bone structure. Hummel and Schutkowski (1986) found that temperatures up to 1000°C resulted in 5% shrinkage in bone length but 27% reduction in cross-sectional bone diameter. Similarly, Thompson's (2005) experimental study on sheep long bones recorded more shrinkage in the epiphyses and attributed this finding to the random arrangement of collagen fibers in trabecular bone. As Thompson (2005) notes, there is a discrepancy in earlier literature regarding which type of bone shrinks more with Gejvall (1969) and Gilchrist and Mytum (1986) arguing that compact bone will shrink the most and McKinley (1994b) and Van Vark (1974) arguing that trabecular bone will exhibit more shrinkage. The author stresses that both arguments may actually be correct: it may be that trabecular bone exhibits more absolute shrinkage but compact bone shows more relative shrinkage.

As mentioned above, the critical temperature at which the degree of heat-induced shrinkage significantly increases has been set at around 800°C (Buikstra and Swegle 1989; Eckert et al. 1988; Holland 1989; Spennemann and Colley 1989). This 800°C threshold lies near the beginning of the fusion stage of heat-induced bone transformation (see above), which is characterised by the coalescence of the inorganic phase and the filling in of the pores left by the freed water and organic phase. This is the process that generates a reduction in bone size (Thompson 2005).

Even though shrinkage can be notable, a more pronounced heat-induced change is warping, that is, a deformity in the natural bone shape (Bontrager and Nawrocki 2015) (Figure 5). Binford (1963) attributed warping to the contraction of muscle fibres, while Spennemann and Colley (1989) linked it to the entrapment of heat inside the medullary cavity. More recently, Thompson (2005) associated warping to the contraction of the periosteum and to the different distribution of collagen within bone. Following the last hypothesis, Gonçalves et al. (2011) argued that warping would depend on bone collagen preservation, thus it would not be related to the presence of soft tissues.

Figure 5. Warped tibia (adapted from Gonçalves et al. 2011 Figure 1)

Discoloration

The varying colors encountered on burned bones have received great attention as color can provide information regarding the temperature of the fire, oxygen availability, the preincineration state of bone, the position of the body on the pyre, and chemical interactions with soil (Bennett 1999; Bennett-Devlin et al. 2006; Binford 1963; Bonucci and Graziani 1975; De Graaff 1961; DeHaan and Nurbakhsh 2001; Hummel et al. 1988; Pope 2007; Shipman et al., 1984; Thompson et al. 2017; Walker et al. 2008; Wärmländer et al. 2019). It must also be remembered that color may be altered by other materials in the firing environment; for example, a proximity to metals may produce green, yellow, pink and red discoloration (Dunlop 1978).

With increasing heat exposure, bone progresses from tan to dark brown to black, then blue, gray, and finally white (Figure 6) (Baby 1954; Bennett 1999; Binford 1963; Buikstra and Swegle 1989; Gilchrist and Mytum 1986; McCutcheon 1992; McKinley 2000; Nicholson 1993; Shipman et al. 1984; Stiner et al. 1995). As thermal damage progresses from the external bone surfaces to the internal ones, colour gradients may be identified across the bone, such as the so-called 'sandwich effect', whereby the external bone surface is white and the internal grey or black (Symes et al. 2015). As briefly discussed in section **Bone response to fire**, when the body is fleshed when exposed to heat, the pugilistic posture (Figure 1) will shield certain anatomical parts and expose others, also leading to patterned color alterations on the skeleton (Symes et al. 2015). Deviations from this expected pattern may offer insights to the pre-incineration condition of the body, e.g. the use of binding or other means that result in an unusual body position in the pyre (McKinley 2015).

The work by Shipman et al. (1984) was the first to standardize burned surface color descriptions using Munsell soil color charts. Since then, different authors have proposed slightly different temperatures at which each color change occurs, even though the progression of colors is largely always the same (e.g. Bonucci and Graziani 1975; Holden et al. 1995a, 1995b; McCutcheon 1992; Munro et al. 2007; Walker et al. 2008).

Figure 6. Bone fragments illustrating color changing sequence from unaltered (far left) to dark brown, black, gray, and white (adapted from Devlin and Herrmann 2013 Figure 16.3)

It must be remembered that heat-induced bone color change is a macroscopic alteration linked to chemical and physical changes in bone structure (Bonucci and Graziani 1975; Devlin and Herrmann 2015; Ellingham et al. 2015; Fairgrieve 2008; McCutcheon 1992; McKinley 2000; Munro et al. 2007; Nicholson 1993; Shipman et al. 1984; Thompson 2004; Thurman and Wilmore 1980). Black color results from the combustion of the organic components of collagen and carbon, while gray and white colors are the outcome of continued combustion that alters the crystalline structure (Devlin and Herrmann 2013). Table 7 summarizes the different colors seen on bones and associated structural changes.

Regarding methods for standardizing color recording, the Munsell Soil Color Chart has been used extensively (Kharkanis et al. 2009; McCutcheon 1992; Munro et al. 2007), following Shipman et al. (1984). Researchers have more recently started investigating the use of the RGB (Red-Green-Blue) colour space and CIE *L*a*B* colour space (a model defined by the Commission Internationale de l'Eclairage, with values for L*: lightness, a*: red-green values, b*: yellow-blue values, which locates color on a three-dimensional axis), together with digital photography and spectrophotometers to enhance objectivity and statistical processing (Devlin and Herrmann 2015; Krap et al. 2019; Ulguim 2015; Walker et al. 2008). Table 8 summarises the strengths and weakeness of these methods.

Table 7. Color change to burned bone and causative factors (adapted from Fairgrieve 2008 Table 3.5 and references therein)

Colour	Causative factors
Brown	Hemoglobin, soil discoloration
Black	Bone carbonization
Gray-blue, gray	Pyrolysis of organic components
White	Bone calcination

Table 8. Advantages and disadvantages of commonly used color recording systems (Thompson et al. 2017 Table 21.2)

Color recording system	Strengths	Weaknesses
Munsell	• Standardised	• Subjective • Difficult to capture surface color variation • Developed for soil color analysis • Difficult for statistical manipulation
RGB	• Standardised • Objective • Quantifiable • Easily comparable	• Requires post-processing or expensive equipment
CIE L*a*B*	• Standardised • Objective • Quantifiable • Easily comparable	• Requires expensive equipment

Depending on the research questions, different recent studies have adopted schemes of coding bone color changes with different levels of detail. Weitzel and McKenzie (2015) simply classified skeletons into two groups: those that exhibited charring (color mostly black) and those that also showed small spots of dark grey, grey and white (colors representing calcination). The location of charring was recorded for each skeletal element and then for the skeleton as a whole, whereby categories were created based on the number of skeletal elements affected by fire as a percentage of the total number of elements present (100%, 75–99%, 50–74%, 25–49% and 0–24% charred). Curtin (2015) adopted a slightly more detailed recording scheme: unburned (no apparent heat-related changes), slight burning (light brown or reddish discoloration, often localised), moderate burning (more extensive dark brown or black discoloration), and severe burning (calcined bone, white, grey or blue-grey in color, often warped and shrunken). Alternative schemes include the categories 'unburned' (no change in color), 'lightly burned' (brown or black, including 'smoked' fragments) or 'heavily burned' (blue-grey or white, also known as 'calcined') (Bontrager and Nawrocki 2015). Color is usually recorded per element or per fragment (Lara et al. 2015). Either all colors visible on each element/fragment or the dominant color may be recorded (Watson et al. 2015).

Fleshed versus dry bone

The issue of distinguishing the pre-incineration state of bones (dry versus fleshed) has been examined by several authors. This issue has implications for both forensic anthropology and bioarchaeological studies, as it provides information about the postmortem treatment of a body/individual. Warping and thumbnail fractures (curved transverse fractures) are among the main attributes adopted in relevant studies. Baby (1954) noted that green (recently defleshed) bone demonstrates warping, whereas dry bone shows no warping but it manifests patina, longitudinal, and transverse fractures. Binford (1963) reported dry bones as having straight transverse cracking, while green bones had curved transverse cracking. Stewart's (1979) findings agreed with those by Binford. However, contrary to the curved transverse fractures noted by Binford (1963), Thurman and Willmore (1980) found that fleshed cremations are characterised by serrated transverse fractures. Etxeberria (1994) found warping occurring only on recently defleshed bones, but not on dry bones. In contrast, Spennemann and Colley (1989) identified warping on an experimentally burned archaeological humerus. This finding was later corroborated by Buikstra and Swegle (1989) who, based on their study of human and animal bones, reported warping in both green and dry bones burned in open-air fires. Similarly, Whyte (2001) found that warping affected fleshed, recently defleshed and dry animal bones that had been experimentally burned. More recently, Gonçalves et al. (2011) found warping in dry human bones burned at a crematorium, lending further support to the fact that this kind of deformity is not exclusively linked to the burning of fleshed or recently defleshed bones. As discussed in Mayne Correia (1997), the disagreement of the results of previous studies can largely be attributed to differences in the experimental methods and the type of skeletal materials adopted, as well as to inconsistencies in terminology.

More recent experimental work by Gonçalves et al. (2015b) explored the frequency of heat-induced warping and thumbnail fractures on cremations of cadavers and skeletons. The authors confirmed that heat-induced warping and thumbnail fractures may occur in dry bones, though they are much more frequent in cadavers (fleshed bodies) than in skeletons. In addition, in burned skeletons, thumbnail fractures were almost thrice as frequent as warping. Therefore, warping is a better indicator of the pre-burning condition of remains.

In addition to the above patterns, remains burned in a wet/fleshed state usually exhibit varying color patterns, deep fracturing and delamination, whereas bones burned in a dry state usually show little color variation, superficial fracturing and limited delamination (Bontrager and Nawrocki 2015). More recently, Lemmers et al. (2020) suggested that evidence of bioerosion lesions can still be identified histologically in burned remains and these can offer important insights to the pre-burning treatment of the body, that is, they can indicate whether the remains had been buried prior to being exposed to heat or not (but see cautionary note by Végh et al. 2021 who discovered that fire may actually produce features that resemble bioerosion).

Weights

During heat exposure, bone mass is reduced due to moisture loss, fat combustion and the breakdown/oxidation of organic molecules (Grupe and Hummel 1991; Thompson 2004, 2005). Several investigations experimentally addressed bone mass reduction using different animal bones burned for different durations and at different temperatures (e.g. Enzo et al. 2007; Grupe and Hummel 1991; Hiller et al. 2003; Munro et al. 2007; Person et al. 1996). Some studies have shown a bone mass loss of 10% up to 200°C, 30% beyond 300°C, and 40% beyond 900°C (Bonucci and Graziani 1975; Grupe and Hummel 1991).

Skeletal weight should always be recorded on burned remains and may often be the only workable data in very fragmentary material. This parameter may allow for some insights especially regarding the completeness of the remains, the degree of anatomical identification and the proportions of each skeletal region (Gonçalves 2011). Relevant studies are largely based on the work of Lowrance and Latimer (1957), who weighed adult skeletons of Asian origin after the bones had been macerated and degreased. They were able to determine the percentage of mass each bone contributed to the total mass of the skeleton. When an anatomical region is underrepresented, it raises issues of selective bone treatment or preservation (André et al. 2013). Trotter and Peterson (1962) studied the relationship between

skeletal mass and the mass of ash. The skeletons used by the authors were macerated, degreased and dried before being heated to 600ºC. The mass lost varied between 30 and 39% depending on the bone (Trotter and Peterson 1962). André et al. (2013) applied Trotter and Peterson's percentages (1962) to Lowrance and Latimer's (1957) data, and calculated new proportions of each bone and each anatomical region (Table 9).

Table 9. Calculation of the theoretical proportions of bones and anatomical regions for a skeleton burned to 600ºC from Trotter and Peterson's data (1962) applied to Lowrance and Latimer's data (1957) (André et al. 2013 Table 2)

		Percentages of bone weights (Lowrance and Latimer 1957)	Bone weights for a skeleton of 2882 g	Percentages of bone weights after burning to 600ºC (Trotter and Peterson 1962)	Bone weights after burning to 600ºC	Percentages of bone weights for a skeleton of 2882 g burned to 600ºC	Percentages of bone weights for each anatomical region (Lowrance and Latimer 1957)	Percentages of bone weights for each anatomical region for a skeleton burned to 600ºC
Head	Cranium	17.98	518.18	67.01	347.22	18.19	20.4	20.7
	Mandible	2.42	69.74	69.71	48.62	2.55		
Trunk	Vertebrae	10.06	289.93	63.96	185.45	9.71	17	16.5
	Ribs	6.42	185.02	64.95	120.17	6.29		
	Sternum	0.47	13.55	62.87	8.52	0.45		
Upper limbs	Scapula	2.84	81.85	65.84	53.89	2.82	17.6	17.8
	Clavicle	1.04	29.97	66.01	19.78	1.04		
	Humerus	6.38	183.87	66.89	122.99	6.44		
	Ulna	2.66	76.66	67.69	51.89	2.72		
	Radius	2.18	62.83	67.59	42.46	2.22		
	Hand bones	2.53	72.91	66.54	48.51	2.54		
Lower limbs	Hip bones	7.83	225.66	64.64	145.87	7.64	45	45
	Femur	17.67	509.25	66.69	339.63	17.79		
	Patella	0.57	16.43	66.2	10.87	0.57		
	Tibia	10.63	306.36	66.92	205.01	10.74		
	Fibula	2.47	71.19	67.64	48.15	2.52		
	Foot bones	5.79	166.87	66	110.13	5.77		

Rather than estimating the weight of individual burned bones or anatomical regions, some researchers have documented it at the full skeleton level in order to assess the completeness of assemblages involving burned human skeletal remains (McKinley 1993; Warren and Maples 1997). The weight of burned remains can be compared to these reference standards to assess their completeness. Such documentation has already been carried out for several populations in Europe (Gonçalves et al. 2013b; Herrmann 1976; Malinowski and Porawski 1969; McKinley 1993), the United States (Bass and Jantz 2004; Van Deest et al. 2011; Warren and Maples 1997) and Asia (Chirachariyavej et al. 2006). Representative data are given in Tables 10-11. The mean skeletal weight of the burned skeletons reported in all those studies presented great variation, which may be the result of different approaches adopted in weighing the remains, or linked to age, sex and regional differences (Bass and Jantz 2004; Chirachariyavej et al. 2006; May 2011; McKinley 1993; McKinley and Bond 2001; Van Deest et al. 2011). Indeed, more aged individuals showed lower weights, and females systematically weighed less than males (Bass and Jantz 2004; Chirachariyavej et al. 2006; Malinowski and Porawski 1969; May 2011). With regard to regional differences, Bass and Jantz (2004) and May (2011) attributed these to regional variation in obesity rates and the body weight of different living populations. Chirachariyavej et al. (2006) further highlighted that different coffins may lead to variation regarding the weight of burned remains since often the coffin ashes are weighted along with the skeletal remains.

Table 10. Mean weight (in grams) for burned skeletal remains per sex (Gonçalves 2011 Table 1.1.2)

Females	Males	Reference
1540	2004	Malinowski and Porawski (1969)
1700	1842	Herrmann (1976)
1616	2284	McKinley (1993)
1840	2893	Warren and Maples (1997)
2350	3379	Bass and Jantz (2004)
2120	2680	Chirachariyavej et al. (2006)
2238	3233	Van Deest et al. (2011)

Table 11. Average weights of burned remains (in grams) in males and females from different archaeological periods (Minozzi 2015 Table 17.3)

Assemblage	Females	Males	Reference
Ligurian Apuans	862	1173	Minozzi (2015)
Borgo Panigale	592	812	Cavazzuti (2008/2010)
Pisa	1061	1255	Bagnoli (2011/2012)
Casinalbo	656	974	Cavazzuti (2008/2010)
German Urn field culture	438	562	Wahl (2015)
German Hallstat/La Tenè	401	572	Wahl (2015)

Additionally to using burned remains' weights to assess the completeness of an assemblage, this method has been adopted to estimate the minimum number of individuals and the sex of an individual (Bass and Jantz 2004; Warren and Maples 1997), although these approaches have serious weaknesses (Fairgrieve 2008; McKinley and Bond 2001). See sections **Minimum Number of Individuals** and **Sex assessment**.

Another application of skeletal weights is related to the reconstruction of the funerary practices of past populations. Reference weights have been used to assess how thoroughly burned remains were collected prior to their deposition in the urn or grave (Gonçalves et al. 2010, 2015b; Holck 1986; McKinley 1994a, 1994b; Murad 1998; Murray and Rose 1993; Richier 2005; Smits 1998). However, this approach does not take into account that not all parts of the skeleton are equally affected by heat-induced weight loss and that many bone fragments exposed to heat can no longer be anatomically identified (Gonçalves 2011).

A general serious limitation of using published weight standards is that such standards have been estimated based on calcined adult (often rather aged) individuals that were burned in modern crematoria. Thus, comparisons with non-calcined, non-adult remains, or remains burned in open pyres is problematic (Thompson et al. 2017).

Recording the weight of burned remains

Despite the limitations associated with the use of burned remains weight, it is important to collect relevant information, at least as a means of quantifying the available material and its preservation (see section Sorting and Cataloguing). For this purpose, the weight of bone per sieve fraction should be obtained, as well as the total weight of bone from the combined sieve fractions. The weight from each sieve fraction should be represented as a percentage of the total weight. Weight in grams should be measured to one decimal place.

Bone microstructure

As already stressed, many of the above presented macroscopic changes are associated with microstructural alterations due to heat exposure. Some broad such alterations are presented in Table 12.

Table 12. Heat-induced bone microstructural alterations (Carroll and Squires 2020)

Category	Temperature	Thin-section micrograph	Description
I	100°C-400°C	1000 μm	well preserved bone microstructure; circular well-formed Haversian systems; unaltered Volkmann's canals, osteons and canaliculi
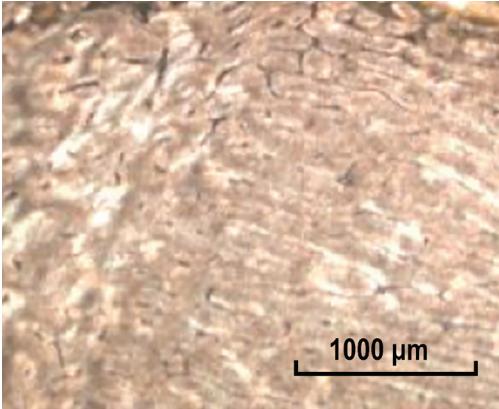
Category	Temperature	Thin-section micrograph	Description
II	500°C-600°C		depletion of organic material; fusion of hydroxyapatite crystals; microfeatures still identifiable, but less well preserved
III	700°C-900°C		more visible degeneration of microscopic features; increased hydroxyapatite fusion; decomposition of all organic material
IV	>1000°C		complete hydroxyapatite fusion → no discernible osteons, Volkmann's canals and canaliculi; few misshaped Haversian systems
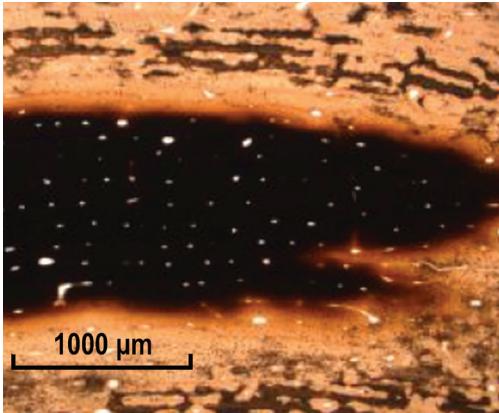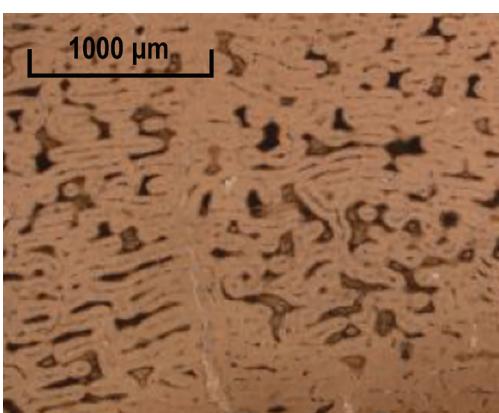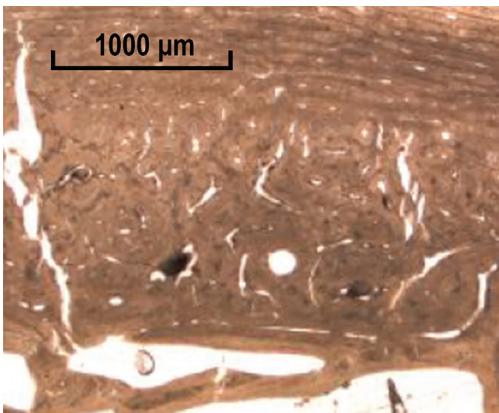
Crystallinity Index

Heat-related variation of the crystallinity index is an important topic examined with regard to the effect of heat on bone mineral structure. When bone is fresh, its crystal structure is poorly ordered, contains small crystals and has a greater strain; un-burned bone, therefore, has a low crystallinity index value (Paschalis et al. 1997; Thompson et al. 2011). When exposed to heating, the crystal structure of bone becomes better ordered and is characterised by larger crystals and less porosity and strain; hence, the crystallinity index value increases (Bartsiokas and Middleton 1992; Figueiredo et al. 2010; Munro et al. 2007; Nagy et al. 2008; Olsen et al. 2008; Shipman et al. 1984; Stiner et al. 2001; Surovell and Stiner 2001; Trueman et al. 2008). Representative Crystallinity indices calculated from XRD (CI) and FTIR (IRSF) data in bones incinerated for 150 mins are given in Table 13.

Table 13. Crystallinity indices at different temperatures calculated from XRD (CI) and FTIR (IRSF) data (drawn from Greiner et al. 2019 Table 3)

Temperature (°C)	CI	IRSF
Unheated	0.11	2.43
100	0.14	2.67
200	0.16	2.81
300	0.17	2.97
400	0.19	3.12
500	0.24	3.56
600	0.35	4.26
700	1.23	6.17
800	1.31	6.32
900	1.28	6.29
1000	1.30	6.96

Regarding the factors underlying the increase in crystallinity index values, Rogers and Daniels (2002) argued that their data support an increase in crystal size as causative factor, but they also stated that a redistribution of existing crystals may also play a role. Hiller et al. (2003) agreed that crystal size indeed increases with heat exposure, but crystal shape and thickness also alter. Person et al. (1996) and, more recently, Sui et al. (2014) stressed the importance of the organic phase in protecting the inorganic phase from change and, therefore, its influence on crystallinity index - although this will only occur up until the loss of the organic phase. Trueman et al. (2008) and Lebon et al. (2010) agreed with these findings and explained them more specifically by highlighting the role of the organic phase in reducing bone porosity, thus crystal surface area exposure to the environment.

Heat-induced changes in bone crystallinity (Etok et al. 2007)
- 25–250°C: loss of poorly bounded water up to 100°C and of structural water from proteins and mineral surface-bound water up to 250°C
- 300–500°C: combustion of about half of the organic phase, increase of crystal size (from ca. 10 to 30 nm) and crystallite thickness (from ca. 2 to 8-9 nm), and formation of new mineral phases
- > 500°C: loss of remaining organic matter, crystallite size enlargement to 110 nm and crystallite thickness growth to 10 nm
- 900°C: loss of intercrystallite space
- > 900°C: formation of β-tricalcium phosphate

Different methods have been used to examine heat-induced bone crystallinity changes: x-ray diffraction (XRD), small-angle x-ray scattering (SAXS), Fourier transform infrared spectrocopy (FTIR), Raman spectroscopy, and others (Mamede et al. 2017; Munro et al. 2007; Sui et al. 2014; Thompson et al. 2009). Crystallinity index values from these methods are not directly comparable, although the general trends they reveal are similar. They all have advantages, but FTIR is preferable because it allows the simultaneous examination of all bone tissue components, it can identify contaminant material and detect substitutions within the elemental structure, it is cost-efficient and more accurate at lower heating temperatures (D'Elia et al. 2007; Paschalis et al. 1997; Wright and Schwarcz 1996). Other scholars advocate XRD over FTIR (Pijoan et al. 2007; Pucéat et al. 2004; Rogers et al. 2010), while others still have used the two approaches in combination (Munro et al. 2007; Pucéat et al. 2004).

Beyond being heat-induced, crystallinity changes also occur naturally after death and are enhanced by weathering (Brock et al. 2010; Piga et al. 2009; Stiner et al. 1995, 2001; Surovell and Stiner 2001). Rogers et al. (2010) examined differences in the microstructural changes that occur in diagenetically altered and burned bones to test whether the two processes can be differentiated. Indeed, the authors identified differences in the lattice order of the mineral of these types of bone, as well as in the directional nature of their microstructure.

When examining crystallinity, it should be remembered that it is not uniform throughout the skeleton (Nakano et al. 2002; Thompson et al. 2009), while age has also been shown to affect it, with younger bone showing lower values than more mature bone (Paschalis et al. 1997). However, Thompson et al. (2011) highlighted the importance of extrinsic variables (e.g., temperature and duration of heat exposure) over intrinsic ones (e.g., skeletal sample location). Moreover, there is evidence that certain pathological conditions can also affect crystallinity index values. Nagy et al. (2008) found a difference in crystallinity index between archaeological remains afflicted by tuberculosis and syphilis. Wright and Schwarcz (1996) also noted that dense enthesophytic bone may be responsible for an unexpected crystallinity index value in their work. Finally, the fire context is also important. Heat from a pyre generally comes from one direction and will cause greater heat-induced crystallinity index changes on the bone surface closest to it (Schurr et al. 2015). Before closing, it must be noted that with appropriate carbonate compensation, increases in crystallinity will still produce a constant crystallinity index (Pucéat et al. 2004).

DNA analysis

A number of studies have highlighted the potential to extract DNA from burned remains once these have been exposed to temperatures up to 600°C (sometimes 300-400°C), at which point much of the organic component is oxidised (Brown et al. 1995; Duffy et al. 1991; Harbeck et al 2011; McKinley 2017; Pusch et al. 2000; Sajantila et al. 1991; Tsuchimochi et al. 2002; Williams et al. 2004). In cases of bone exposure to higher temperatures and/or for long duration, such as in modern commercially cremated remains, experimental and case studies indicate DNA cannot be retrieved (Cattaneo et al. 1999; Nelson and Melton 2007; Rees and Cox 2010; von Wurmb-Schwark et al. 2004).

Stable and radiogenic isotope analysis

Among the earliest experimental studies on the applicability of stable isotope analysis on burned skeletal remains, DeNiro et al. (1985) found that boiling or roasting did not change the $\delta^{13}C$ and $\delta^{15}N$ values by more than 1‰; however, more extreme heating altered $\delta^{13}C$ and $\delta^{15}N$ values by as much as 5‰ and 4‰, respectively. More recently, Schurr et al. (2015) confirmed that stable nitrogen isotope ratios are significantly affected by heating; however, contrary to DeNiro et al. (1985), $\delta^{13}C$ values did not change particularly by heating, although in burned samples they showed increased scatter around the mean value of −13.2 ± 0.1‰. For oxygen isotopes, Munro et al. (2007) found that $\delta^{18}O_p$ values were preserved at temperatures lower than 300°C; however, at higher temperatures, values were up to 7‰ smaller. In their experimental work, Harbeck et al. (2011) concluded that stable isotopic values of the light elements carbon, nitrogen and oxygen are unaltered up to 200°C, but over this temperature, results are unreliable. These results disagree with a recent experimental study by Robinson and Kingston (2020) who tested the effect of heating on faunal $\delta^{13}C_{enamel}$ and $\delta^{18}O_{enamel}$ and found that although $\delta^{18}O$ values are significantly altered from 300°C onwards, $\delta^{13}C$ values are minimally affected at temperatures as high as 1100°C (except in thin-enameled species). Stable isotopic values of the heavy element strontium also remain unchanged up to 1000°C, as supported in experimental studies (Snoeck et al. 2015) and case studies using archaeological material (Graham and Bethard 2019;

Snoeck et al. 2016, 2018; Taylor et al. 2020). In this direction, the work by Harvig et al. (2014) showed that strontium isotope ratios estimated from the otic capsule of the petrous part of the temporal bone show a high correlation with ratios obtained from the dental enamel of the same individuals, in burned and unburned remains. Hence, the petrous bone can substitute dental enamel where the latter is too fragmented.

The validity of radiocarbon dating of burned bones has been supported by different studies (Minami et al. 2019; De Mulder et al. 2007, 2012; Naysmith et al. 2007; Olsen et al. 2008, 2011). However, in several cases charred bones exhibit aberrant results, likely due to post-depositional CO_3 substitution (Olsen et al. 2008; Van Strydonck et al. 2009). Contrary to charred remains, in calcined bones, the compactness of the bone structure prevents carbonate substitution (Van Strydonck et al. 2005). Thus, dating should employ calcined bone rather than charred one (Lanting et al. 2001). A serious potential limitation in radiocarbon dating is the so-called 'old wood effect', that is, we may be dating the wood used for the cremation pyre rather than the skeletal remains (Geyh 2001; Olsen et al. 2013; Rose et al. 2020; Snoeck et al. 2014; Van Strydonck et al. 2010; Zazzo et al. 2012).

Heat-induced dental alterations

As with bone, many extrinsic variables control the effect of heat on teeth, such as temperature, duration of exposure, state of the body before exposure, and others. Nonetheless, some broad patterns can be outlined. During fire exposure, different teeth and dental tissues are differentially affected. The anterior teeth may be less affected compared to the posterior teeth if they fall out at an early stage of the burning process; once they are on the ground, they are likely below or away from the fire. However, if they do not fall out, the enamel of the anterior teeth is more affected by heat exposure than that of the molars because the latter are better protected by the orofacial tissues (Delattre 2000; Sakoda et al. 2000). Posterior teeth are generally rather protected and their crown fragmentation is more predictable than that of anterior teeth, with cracks appearing first along the grooves that separate the cusps (Schmidt 2015). An early but seminal study on the effect of heat on dental tissues was by Harsányi (1976). The key findings regarding heat-induced macroscopic and microscopic alterations to enamel and dentin are presented in Tables 14-15. Shipman et al. (1984) also systematically explored microscopic heat-induced dental changes, as summarised in Tables 16-17.

Table 14. Macroscopic and microscopic effects on enamel of one-hour heat exposure at different temperatures (drawn from Harsányi 1976; reprinted by Fairgrieve 2008 Table 7.2)

°C	Macroscopic changes	Microscopic changes
200	Color changes	None
300	Dark grayish brown color; enamel starts to peel off via small crevices	Small crevices; enamel intact between crevices
500	Gray color; longitudinal furrows	Crevice network; multiangular plates
700	Light grayish-white color; fragmentation	Fine grained granules; original surface unrecognizable
900	Almost white color; more pronounced fragmentation	Fusion of enamel grains; unrecognizable structure
1000	Porcelain-white color	"Structureless" smooth plates
1100	Porcelain-white color; fragmentation	Same as at 1000°C
1300	Tiny smooth porcelain-white fragments with glass-like surface	Inorganic salts fused into round formations

Table 15. Macroscopic and microscopic effects on dentin of one-hour heat exposure at different temperatures (drawn from Harsányi 1976; reprinted by Fairgrieve 2008 Table 7.5)

°C	Macroscopic changes	Microscopic changes
200	Color changes	None
300	Light grayish-brown color	Structure preserved; tubules opened horizontally or longitudinally; morphology unaffected
500	Dark grayish-black color; pulp chamber and root canal preserved	Preserved-open dental canalicules, no narrowing
700	Pale gray color; parts of pulp chamber and root canal recognizable but narrowed	Tubules narrowed but visible; peritubular zone heat-resistant relative to intertubular dentin
900	Almost white color; large pieces with root present	Narrowed dentin tubules 1.5 to 1.7 µm in diameter; anastomoses between tubules not visible
1000	Porcelain-white color; narrowed pulp chamber; root canal slightly distinguishable	Tubular structure preserved; minute "pearls" of material in string formation
1100	Porcelain-white root color; narrowed pulp chamber and root canal still observable	Tubular structure preserved; narrow portions and anastomoses not observable; round plates and granules of varying size
1300	Minute porcelain-white fragments; remains of narrowed pulp chamber and root canal may be observable	Structures decomposed and fused into granules of varying size

Table 16. Microscopic heat-induced alterations to enamel (drawn from Shipman et al. 1984; reprinted by Fairgrieve 2008 Table 7.3)

Stage I	20-185°C: enamel normal
Stage II	185-285°C: dimples develop, but overall surface texture smoother than in Stage I
Stage III	285-440°C: rounded particles form and cover the surface
Stage IV	440-800°C: vitrified or glassy particles separated by pores and fissures; enamel close to the CEJ breaks up
Stage V	800-940°C: fine particles of stage IV coalesce into larger, smooth-surfaced globules that fuse into an irregularly-shaped mass pierced by rounded holes

Table 17. Microscopic heat-induced alterations to dentin (drawn from Shipman et al. 1984; reprinted by Fairgrieve 2008 Table 7.6)

Stage I	20-185°C: dentinal surface of pulp cavity normal; calcospherites clearly visible and pierced by smooth-edged, circular openings to the dentinal tubules
Stage II	185-285°C: peritubular matrix shrunken and separated from intertubular matrix; surface of intertubular matrix showing small asperities that produce roughened texture
Stage III	285-440°C: asperities of stage II have melted and smoothed out; division between peritubular and intertubular matrix rarely visible; elongated openings of dentinal tubules; intertubular matrix forming a network of bars between openings
Stage IV	440-800°C: appearance of many particles which create frothy or fleecy texture; increasing elongation and enlargement of tubule openings; some areas of glassy texture, perforated by irregularly-shaped openings
Stage V	800-940°C: frothy protuberances of stage IV have coalesced into globules that fuse into nodular spikes; spaces between spikes are remnants of tubules and spikes are remnants of intertubular bars

A series of recent experimental studies by Sandholzer and his colleagues (Sandholzer 2015; Sandholzer et al. 2013, 2014a, 2014b) complemented these earlier works and found that the enamel was fully preserved and attached to the dentin at 400°C, with small cracks visible in the crown and multiple small cracks in the root. Between 500°C and 700°C the enamel was partially separated from the coronal dentin or fragmented; deep cracks were present in the root, and small cracks on the enamel surface, with the majority appearing in the dentin-enamel junction. At temperatures above 800°C, the enamel and dentin were separated and fragmented.

Recent studies have also examined systematically color changes in the tooth crown and root (Figure 7). Changes in the enamel are subtle, from natural pale yellow color to pale brown, light grey and white (Beach et al. 2015). Heat-related color changes in roots go from pale yellow to black, brown, greyish-blue, light grey, chalky-white and, finally, white-pink (Beach et al. 2015; Fairgrieve 2008; Sandholzer et al. 2013). It must be noted that the part of the root that lies inside the socket during heat exposure is better protected, and its color will often differ from that of the exposed part of the root (Schmidt 2015).
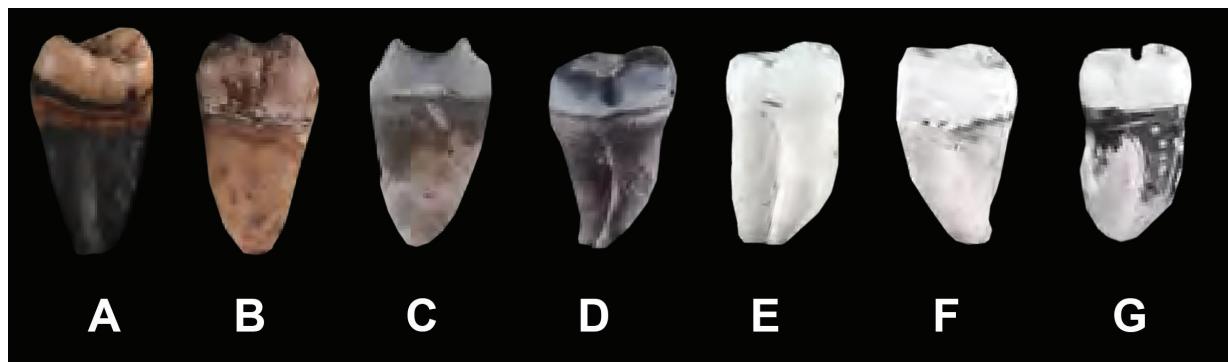
Figure 7. Color alteration of human teeth after 30-minute heat exposure at 400°C (A) to 1000°C (G) (adapted from Sandholzer 2015 Figure 21.1)

Important dimensional changes also take place during dental exposure to heat, as is the case with bones. Sandholzer (2015) and Sandholzer et al. (2013) found mean dentinal shrinkage in tooth roots to be between 4.78% (at 400°C) and 32.53% (at 1000°C), showing a sharp increase between 700°C and 800°C (11.5–24.2%) (Table 18). Similarly, Beach et al. (2015) examined the degree of weight loss at different temperatures and for different durations of exposure, and the results are summarised in Table 19.

Table 18. Mean dentinal volume shrinkage at different temperatures after constant 30-minute exposure (Sandholzer et al. 2013 Table 1)

Temperature (°C)	Shrinkage (% ± 1 SD)
400	4.78 ± 0.80
500	5.94 ± 1.36
600	8.66 ± 0.83
700	11.53 ± 1.53
800	24.20 ± 4.23
900	27.50 ± 4.35
1000	32.53 ± 5.35

Table 19. Average percentage weight loss for teeth at different temperatures after constant 30- and 60-minute exposure (Beach et al. 2015 Table 7.2)

Temperature (°C)	Average percentage weight loss at 30 min	Average percentage weight loss at 60 min
204	16.3	13.1
260	17.3	17.3
316	13.3	23.1
371	16.9	21.3
427	37.9	22.5
482	25.1	30.9
538	27.4	24.1
593	36.0	33.3

The stage of development of a tooth needs to be taken into consideration when examining the effect of fire. Silva et al. (2009) found that in teeth with more than two thirds of the crown formed, a clear distinction may be seen between the forming enamel that has higher organic content, and more completely mineralised enamel. Similarly, it is important to consider if teeth are deciduous or permanent. Most of the abovementioned research examined permanent teeth. An important study focused on the deciduous dentition is by Karkhanis et al. (2009); the results are summarized in Table 20 and partly visualized in Figure 8.

Table 20. Heat-induced changes in deciduous teeth (Karkhanis et al. 2009 Table 1)

°C	Color	Stereomicroscopic and SEM traits
100	• Crown: pale yellow, very pale brown • Root: yellowish brown	• Crown fracturing in anterior teeth • Surface crazing • Melting of external surface
200	• Crown: pale yellow, gray • Cervical patches: very dark brown • Root: shiny black	• Surface bubbling and vesicle formation on root surface • Silvery deposits on root surface
300	• Crown: light gray • Patches: very dark gray • Root: shiny black	• Surface bubbling on root surface • Globular knob-like formations on predentinal surface
400	• Enamel: very pale brown • Patches: very dark brown • Dentin: very dark gray • Cementum: light yellowish brown	• Initial separation of enamel and dentin • Deep fissures on root surface and through dentin
500	• Enamel: light gray • Patches: dark gray • Dentin: dark bluish gray • Cementum: grayish brown, light grayish brown	• Crown-root separation • Complete separation of enamel and dentin • Loss of enamel lustre • Reduction in tubular diameter, especially near dentino-enamel junction
600	• Enamel: light gray • Cervical patches: very dark gray • Dentin: dark bluish gray • Cementum: bluish black	• Extreme fragility; deep fissures in dentin and cementum

| °C	Color	Stereomicroscopic and SEM traits
700	• Enamel: light bluish gray • Dentin: dark bluish gray • Cementum: light bluish black	• Extreme reduction in dentinal tubule diameter
800	• Enamel: bluish gray • Dentin: very dark bluish gray • Cementum: very dark bluish gray	• Specular appearance in predentinal surface
900	• Enamel: neutral white • Dentin: light bluish gray • Cementum: light bluish gray • Patches: very dark bluish gray	• Star-shaped fibrillar structures emerging from intertubular dentin matrix • Cementum unidentified, with granular appearance
1000	• Enamel: light bluish gray • Dentin: light bluish gray • Cementum (external): bluish black • Cementum (subsurface): light bluish gray	• Obliteration of dentinal tubules • Identifiable prismatic structure of enamel and tubular morphology of dentin
1100	• Enamel/dentin/cementum: light bluish gray • Predentin: light greenish gray, pink discoloration of the crown	• Identifiable enamel and dentin • Granular appearance of intertubular dentin • Cementum unidentifiable, with granular appearance
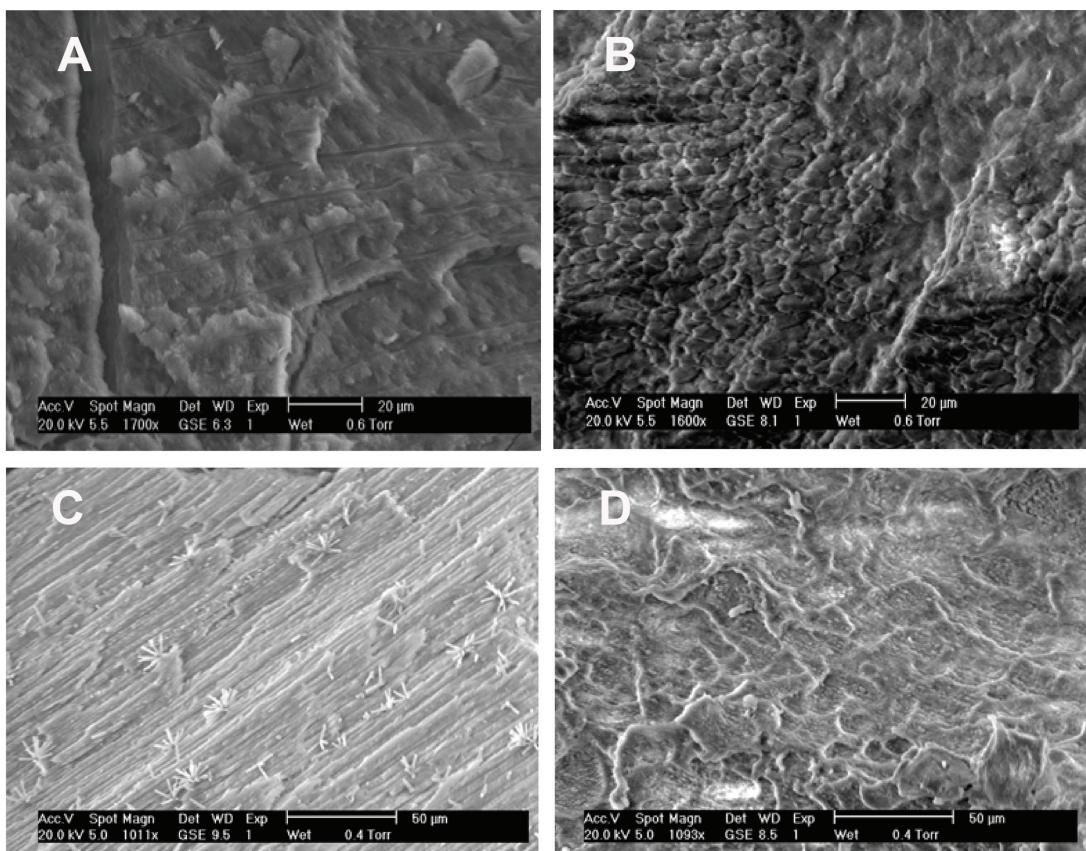
Figure 8. SEM images of deciduous tooth alteration after heat exposure. A. dentin after exposure to 500°C for 30 mins, B. enamel subsurface after exposure to 700°C for 30 mins (note prismatic structure), C. dentin after exposure to 900°C for 30 mins (note star-shaped crystals), D. cementum after exposure to 900°C for 30 mins (note melted surface) (Karkhanis et al. 2009 Figures 2-3 and 6-7)

REFERENCES

Absolonova K, Veleminsky P, Dobisikova M, Beran M, Zocova J. 2013. Histological estimation of age at death from the compact bone of burned and unburned human ribs. *Journal of Forensic Sciences* 58: S135-145

Adams BJ, Konigsberg LW. 2004. Estimation of the most likely number of individuals from commingled human skeletal remains. *American Journal of Physical Anthropology* 125: 138-151

Amarante A, Ferreira MT, Makhoul C, Vassalo AR, Cunha E, Gonçalves D. 2019. Preliminary results of an investigation on postmortem variations in human skeletal mass of buried bones. *Science and Justice* 59: 52-57

André A, Leahy R, Rottier S. 2013. Cremated human remains deposited in two phases: evidence from the necropolis of the Tuileries site (Lyon, France: 2nd century AD). *International Journal of Osteoarchaeology* 25: 489-501

Baby RS. 1954. *Hopewell cremation practices.* Columbus, Ohio: Ohio Historical Society

Bagnoli J. 2011/2012. *Studio dei resti cremati umani provenienti dalla necropoli villanoviana di via Marche a Pisa.* Tesi di Scuola di Specializzazione in Beni Archeologici, Università di Pisa

Bartsiokas A, Middleton AP. 1992. Characterization and dating of recent and fossil bone by X-ray diffraction. *Journal of Archaeological Science* 19: 63–72

Bass WM. 1984. *Is it possible to consume a body completely in a fire?* In: Rathbun TA, Buikstra JE (eds.) Human identification: Case studies in forensic anthropology. Springfield, IL: Charles C. Thomas; pp. 159–167

Bass WM, Jantz RL. 2004. Cremation weights in East Tennessee. *Journal of Forensic Sciences* 49: 901-904

Beach JJ, Passalacqua NV, Chapman EN. 2015. *Heat-related changes in tooth color.* In: Schmidt CW, Symes SA (eds.) The analysis of burned human remains, 2nd edition. Amsterdam: Elsevier; pp. 139-147

Bennett JL. 1999. Thermal alteration of buried bone. *Journal of Archaeological Science* 26: 1–8

Bennett-Devlin J, Kroman A, Herrmann NP, Symes S. 2006. Time temperature and color: heat intensity versus exposure duration. Part 1. Macroscopic influence on burned bone. *Proceedings of the American Academy of Forensic Sciences* 12: 311–312

Binford LR. 1963. An analysis of cremations from three Michigan sites. *Wisconsin Archaeologist* 44: 98–110

Bohnert M, Rost T, Pollak S. 1998. The degree of destruction of human bodies in relation to the duration of the fire. *Forensic Science International* 95: 11–21

Bontrager AB, Nawrocki SP. 2015. *A taphonomic analysis of human cremains from the Fox Hollow Farm serial homicide site.* In: Schmidt CW, Symes SA (eds.) The analysis of burned human remains, 2nd edition. Amsterdam: Elsevier; pp. 229-245

Bonucci E, Graziani G. 1975. Comparative thermogravimetric, X-ray diffraction and electron microscope investigations of burnt bones from recent, ancient and prehistoric age. *Atti Memorie Accademia Nazionale die Lincei, Scienze Fisiche, Matematiche e Naturali* 59: 517–534

Bradtmiller B, Buikstra JE. 1984. Effects of burning on human bone microstructure: A preliminary study. *Journal of Forensic Sciences* 29: 535-540

Brickley MB. 2007. *A case of disposal of a body through burning and recent advances in the study of burned human remains.* In: Brickley MB, Ferllini R (eds.) Forensic anthropology: Case sudies from Europe. Springfield, IL: Charles C. Thomas; pp. 69–85

Brock F, Higham T, Bronk Ramsey C. 2010. Pre-screening techniques for identification of samples suitable for radiocarbon dating of poorly preserved bones. *Journal of Archaeological Science* 37: 855–865

Brown KA, O'Donoghue K, Brown TA. 1995. DNA in cremated bones from an Early Bronze Age cemetery cairn. *International Journal of Osteoarchaeology* 5: 181-187

Buikstra JE, Swegle M. 1989. *Bone modification due to burning: experimental evidence.* In: Bonnichsen R, Sorg MH (eds.) Bone modification. University of Maine, Orono: Center for the Study of the First Americans; pp. 247–258

Byers SN. 2005. *Introduction to forensic anthropology, 2nd edition.* Toronto: Pearson

Carroll EL, Squires KE. 2020. Burning by numbers: A pilot study using quantitative petrography in the analysis of heat-induced alteration in burned bone. *International Journal of Osteoarchaeology* 30: 691–699

Cattaneo C, DiMartino S, Scali S, Craig OE, Grandi M, Sokol RJ. 1999. Determining the human origin of fragments of burnt bone: a comparative study of histological, immunological and DNA techniques. *Forensic Science International* 102: 181–191

Cavazzuti C. 2008/2010. *Aspetti rituali, sociali e paleodemografici di alcune necropoli protostoriche a cremazione dell'Italia Settentrionale.* Tesi Dottorato di Ricerca in Scienze e Tecnologie per l'Archeologia e i Beni Culturali, Università di Ferrara

Cavazzuti C, Bresadola B, d'Innocenzo C, Interlando S, Sperdutil A. 2019. Towards a new osteometric method for sexing ancient cremated human remains. Analysis of Late Bronze Age and Iron Age samples from Italy with gendered grave goods. *PLoS ONE* 14: e0209423

Chan AH, Crowder CM, Rogers TL. 2007. Variation in cortical bone histology within the human femur and its impact on estimating age at death. *American Journal of Physical Anthropology* 132: 80-88

Chirachariyavej T, Amnueypol C, Sanggarnjanavanich S, Tiensuwan M. 2006. The relationship between bone and ash weight to age, body weight and body length of Thai adults after cremation. *Journal of the Medical Association of Thailand* 89: 1940-1945

Christensen AM. 2002. Experiments in the combustibility of the human body. *Journal of Forensic Sciences* 47: 466–470

Collini F, Amadasi A, Mazzucchi A, Porta D, Regazzola VL, Garofalo P, Di Blasio A, Cattaneo C. 2015. The erratic behavior of lesions in burnt bone. *Journal of Forensic Sciences* 60: 1290-1294

Costamagno S, Théry-Parisot I, Brugal J-P, Guibert R. 2005. *Taphonomic consequences of the use of bones as fuel. Experimental data and archaeological applications.* In: O'Connor T (ed.) Biosphere to lithosphere: New studies in vertebrate taphonomy. Oxford: Oxbow Books; pp. 51-62

Curtin JA. 2015. *Putting together the pieces: Reconstructing mortuary practices from commingled ossuary cremains.* In: Schmidt CW, Symes SA (eds.) The analysis of burned human remains, 2nd edition. Amsterdam: Elsevier; pp. 219-227

D'Elia M, Gianfrate G, Quarta G, Giotta L, Giancane G, Calcagnile L. 2007. Evaluation of possible contamination sources in the 14C analysis of bone samples by FTIR spectroscopy. *Radiocarbon* 49: 201-210

Davies DJ, Mates LH. 2005. *Encyclopaedia of cremation.* Aldershot: Ashgate

De Graaff G. 1961. Gross effects of a primitive hearth. *South African Archaeological Bulletin* 16: 25–26

de Gruchy S, Rogers TL. 2002. Identifying chop marks on cremated bone: a preliminary study. *Journal of Forensic Sciences* 47: 933-936

DeHaan J. 2002. *Kirk's fire investigation, 5th edition*. Upper Saddle River, NJ: Prentice Hall

DeHaan JD. 2012. Sustained combustion of bodies: some observations. *Journal of Forensic Sciences* 57: 1578-1584

DeHaan JD. 2015. *Fire and bodies.* In: Schmidt CW, Symes SA (eds.) The analysis of burned human remains, 2nd edition. Amsterdam: Elsevier; pp. 1-15

DeHaan J, Nurbakhsh S. 2001. Sustained combustion of an animal carcass and its implications for the consumption of human bodies in fires. *Journal of Forensic Sciences* 46: 1076-1081

Delattre VF. 2000. Burned beyond recognition: systematic approach to the dental identification of charred human remains. *Journal of Forensic Sciences* 45: 589-596

De Mulder G, Van Strydonck M, Boudin M, Leclercq W, Paridaens N, Warmenbol E. 2007. Re-evaluation of the Late Bronze Age and Early Iron Age chronology of the Western Belgian urnfields based on 14C dating of cremated bones. *Radiocarbon* 49: 499-514

De Mulder G, Van Strydonck M, Annaert R, Boudin M. 2012. A Merovingian surprise: Early Medieval radiocarbon dates on cremated bone (Borsbeek, Belgium). *Radiocarbon* 54: 581-588

DeNiro MJ, Schoeninger MJ, Hastorf CA. 1985. Effect of heating on the stable carbon and nitrogen isotope ratios of bone collagen. *Journal of Archaeological Science* 12: 1-7

Devlin JB, Herrmann NP. 2013. *Taphonomy of fire.* In: Tersigni-Tarrant MTA, Shirley NR (eds.) Forensic anthropology: an introduction. Boca Raton: CRC Press; pp. 307-323

Devlin JB, Herrmann NP. 2015. *Bone colour.* In: Schmidt CW, Symes SA (eds.) The analysis of burned human remains, 2nd edition. Amsterdam: Elsevier; pp. 119-138

Dokládal M. 1971. *A further contribution to the morphology of burned bones.* In: Novotny N (ed.) Proceedings of the Anthropological Congress dedicated to Aleš Hrdlička. Prague: Czechoslavak Academy of Sciences; pp. 561–568

Duffy JB, Waterfield JD, Skinner MF. 1991. Isolation of tooth pulp cells for sex chromatin studies in experimental dehydrated and cremated remains. *Forensic Science International* 49: 127–141

Dunlop JM. 1978. Traffic light discoloration in cremated bones. *Medicine, Science and the Law* 18: 163-173

Eckert WG, James S, Katchis S. 1988. Investigation of cremations and severely burned bodies. *American Journal of Medicine and Pathology* 9: 188–200

Ellingham STD, Thompson TJU, Islam M, Taylor G. 2015. Estimating temperature exposure of burnt bone – A methodological review. *Science and Justice* 55: 181–188

Enzo S, Bazzoni M, Mazzarello V, Piga G, Bandiera P, Melis P. 2007. A study by thermal treatment and X-ray powder diffraction on burnt fragmented bones from tombs II, IV and IX belonging to the hypogeic necropolis of ''Sa Figu'' near Ittiri, Sassari (Sardinia, Italy). *Journal of Archaeological Science* 34: 1731-1737

Etok SE, Valsami-Jones E, Wess TJ, Hiller JC, Maxwell CA, Rogers KD, Manning DAC, White ML, Lopez-Capel E, Collins MJ, Buckley M, Penkman KEH, Woodgate SL. 2007. Structural and chemical changes of thermally treated bone apatite. *Journal of Materials Science* 42: 9807–9816

Etxeberria F. 1994. Aspectos macroscópicos del hueso sometido al fuego: revisión de las cremaciones descritas en el País Vasco desde la arqueologia. *Munibe* 46: 111–116

Fairgrieve SI. 2008. *Forensic cremation. Recovery and analysis.* Boca Raton: CRC Press

Fazekas IG, Kósa F. 1978. *Forensic fetal osteology.* Budapest: Akedémiai Kiadó

Figueiredo M, Fernando A, Martins G, Freitas J, Judas F, Figueiredo H. 2010. Effect of the calcination temperature on the composition and microstructure of hydroxyapatite derived from human and animal bone. *Ceramics International* 36: 2383–2393

Franceschetti L, Mazzucchi A, Magli F, Collini F, Gaudio D, Cattaneo C. 2021. Are cranial peri-mortem fractures identifiable in cremated remains? A study on 38 known cases. *Legal Medicine* 49: 101850

García-Donas JG, Dyke J, Paine RR, Nathena D, Kranioti EF. 2016. Accuracy and sampling error of two age estimation techniques using rib histomorphometry on a modern sample. *Journal of Forensic and Legal Medicine* 38: 28-35

Geber J, Hensey R, Meehan P, Moore S, Kador T. 2017. Facilitating transitions: Postmortem processing of the dead at the Carrowkeel Passage Tomb Complex, Ireland (3500-3000 cal B.C.). *Bioarchaeology International* 1: 35-51

Gejvall NG. 1969. *Cremations.* In: Brothwell D, Higgs E (eds.) Science in archaeology. London: Thames and Hudson; pp. 468-479

Geyh M. 2001. Bomb 14C dating of animal tissues and hair. *Radiocarbon* 43: 723-730

Gilchrist M, Mytum H. 1986. Experimental archaeology and burnt animal bone from archaeological sites. *Circaea* 4: 29-38

Gocha TP, Schutkowski H. 2013. Tooth cementum annulation for estimation of age-at-death in thermally altered remains. *Journal of Forensic Sciences* 58(S1): 151-155

Godinho RM, Gonçalves D, Valera AC. 2019a. The pre-burning condition of Chalcolithic cremated human remains from the Perdigões enclosures (Portugal). *International Journal of Osteoarchaeology* 29: 706-717

Godinho RM, Oliveira-Santos I, Pereira MFC, Maurício A, Valera A, Gonçalves D. 2019b. Is enamel the only reliable hard tissue for sex metric estimation of burned skeletal remains in biological anthropology? *Journal of Archaeological Science: Reports* 26: 101876

Gonçalves DM. 2011. *The value of quantitative analysis for the bioanthropological research of burned human skeletal remains.* PhD thesis, University of Coimbra

Gonçalves D, Duarte C, Costa C, Muralha J, Campanacho V, Costa AM, Angelucci DE. 2010. The Roman cremation burials of Encosta de Sant'Ana (Lisbon). *Revista Portuguesa de Arqueologia* 13: 125–144

Gonçalves D, Thompson TJU, Cunha E. 2011. Implications of heat-induced changes in bone on the interpretation of funerary behaviour and practice. *Journal of Archaeological Science* 38: 1308-1313

Gonçalves D, Thompson TJU, Cunha E. 2013a. Osteometric sex determination of burned human skeletal remains. *Journal of Forensic and Legal Medicine* 20: 906-911

Gonçalves D, Cunha E, Thompson TJU. 2013b. Weight references for burned human skeletal remains from Portuguese samples. *Journal of Forensic Sciences* 58: 1134-1140

Gonçalves D, Thompson TJU, Cunha E. 2015a. Sexual dimorphism of the lateral angle of the internal auditory canal and its potential for sex estimation of burned human skeletal remains. *International Journal of Legal Medicine* 129: 1183-1186

Gonçalves D, Cunha E, Thompson TJU. 2015b. Estimation of the pre-burning condition of human remains in forensic contexts. *International Journal of Legal Medicine* 129: 1137-1143

Gouveia MF, Santos IO, Santos AL, Gonçalves D. 2017. Sample-specific odontometric sex estimation: A method with potential application to burned remains. *Science & Justice* 57: 262-269

Graham DG, Bethard JD. 2019. Reconstructing the origins of the Perrins Ledge cremains using strontium isotope analysis. *Journal of Archaeological Science: Reports* 24: 350–362

Greiner M, Rodríguez-Navarro A, Heinig MF, Mayer K, Kocsis B, Göhring A, Toncala A, Grupe G, Schmahl WW. 2019. Bone incineration: An experimental study on mineral structure, colour and crystalline state. *Journal of Archaeological Science: Reports* 25: 507-518

Grupe G, Herrmann B. 1983. Über das Schrumpfungsverhalten Experimentell Verbrannter Spongiöser Knochen am Beispiel des Caput Femoris. *Zeitschrift für Morphologie und Anthropologie* 74: 121–127

Grupe G, Hummel S. 1991. Trace element studies on experimentally cremated bone. I. Alteration of the chemical composition at high temperatures. *Journal of Archaeological Science* 18: 177-186

Guo E. 2001. *Mechanical properties of cortical bone and cancellous bone tissue.* In: Cowin SC (ed.) Bone mechanics handbook, 2nd edition. Boca Raton: CRC Press; pp. 10.11-10.23

Harbeck M, Schleuder R, Schneider J, Wiechmann I, Schmahl WW, Grupe G. 2011. Research potential and limitations of trace analyses of cremated remains. *Forensic Science International* 204: 191–200

Harsányi L. 1976. Scanning electron microscopic investigation of thermal damage of the teeth. *Acta Morphologica Academiae Scientiarium Hungaricae* 23: 271–281

Harsányi L. 1993. *Differential diagnosis of human and animal bone.* In: Grupe G, Garland AN (eds.) Histology of ancient bone: methods and diagnosis. Berlin: Springer; pp. 79–94

Harvig L, Lynnerup N. 2013. On the volume of cremated remains - a comparative study of archaeologically recovered cremated bone volume as measured manually and assessed by Computed Tomography and by Stereology. *Journal of Archaeological Science* 40: 2713-2722

Harvig L, Frei KM, Price TD, Lynnerup N. 2014. Strontium isotope signals in cremated petrous portions as indicator for childhood origin. *PLoS ONE* 9: e101603

Heglar R. 1984. *Burned remains.* In: Rathbun TA, Buikstra JE (eds.) Human identification: Case studies in forensic anthropology. Springfield, IL: Charles C. Thomas; pp. 148-158

Herrmann B. 1976. Neuere Ergebnisse zur Beurteilung menschlicher Brandknochen. *Zeitschrift für Rechtsmedizin* 77: 191–200

Herrmann B. 1977. On histological investigations of cremated human remains. *Journal of Human Evolution* 6: 101-103

Herrmann NP, Bennett JL. 1999. The differentiation of traumatic and heat-related fractures in burned bone. *Journal of Forensic Sciences* 44: 461–469

Higgins OA, Vazzana A, Scalise LM, Riso FM, Buti L, Conti S, Bortolini E, Oxilia G, Benazzi S. 2020. Comparing traditional and virtual approaches in the micro-excavation and analysis of cremated remains. *Journal of Archaeological Science: Reports* 32: 102396

Hiller JC, Thompson TJU, Evison MP, Chamberlain AT, Wess TJ. 2003. Bone mineral change during experimental heating: an X-ray scattering investigation. *Biomaterials* 24: 5091–5097

Holck P. 1986. *Cremated bones: A medical-anthropological study of an archaeological material on cremation burials.* Oslo: Anatomisk Institutt Universitetet

Holden JL, Phakey PP, Clement JG. 1995a. Scanning electron microscope observations of heat-treated human bone. *Forensic Science International* 74: 29-45

Holden JL, Phakey PP, Clement JG. 1995b. Scanning electron microscope observations of incinerated human femoral bone: a case study. *Forensic Science International* 74: 17-28

Holland TD. 1989. Use of the cranial base in the identification of fire victims. *Journal of Forensic Sciences* 34: 458–460

Holland TD. 1992. Estimation of adult stature from fragmentary tibias. *Journal of Forensic Sciences* 37: 1223–1229

Hummel S, Schutkowski H. 1986. Das Verhalten von Knochengewebe unter dem Einfluss höherer Temperaturen, Bedeutungen für die Leichenbranddiagnose. *Zeitschrift für Morphologische Anthropologie* 77: 1–9

Hummel S, Schutkowski H, Herrmann B. 1988. Advances in cremation research. *Actes des 3ème Journées Anthropologiques* 24: 177–194

Huxley AK. 1998. Analysis of shrinkage in human fetal diaphyseal lengths from fresh to dry bone using Petersohn and Köhler's data. *Journal of Forensic Sciences* 43: 423–426

Huxley AK, Kósa F. 1999. Calculation of percent shrinkage in human fetal diaphyseal lengths from fresh bone to carbonized and calcined bone using Petersohn and Köhler's data. *Journal of Forensic Sciences* 44: 577-583

Irish JD, Potter BA, Reuther JD. 2015. *An 11,500-year-old human cremation from Eastern Beringia (Central Alaska).* In: Schmidt CW, Symes SA (eds.) The analysis of burned human remains, 2nd edition. Amsterdam: Elsevier; pp. 295-306

Karkhanis S, Ball J, Franklin D. 2009. Macroscopic and microscopic changes in incinerated deciduous teeth. *Journal of Forensic Odontostomatology* 27: 9-19

Knüsel CJ, Outram AK. 2004. Fragmentation: the zonation method applied to fragmented human remains from archaeological and forensic contexts. *Environmental Archaeology* 9: 85-98

Kooi RJ, Fairgrieve SI. 2013. SEM and stereomicroscopic analysis of cut marks in fresh and burned bone. *Journal of Forensic Sciences* 58: 452-458

Krap T, Ruijter JM, Nota K, Karel J, Burgers AL, Aalders MCG, Oostra R-J, Duijst W. 2019. Colourimetric analysis of thermally altered human bone samples. *Scientific Reports* 9: 8923

Lagacé F, Verna E, Adalian P, Baccino E, Martrille L. 2019. Testing the accuracy of a new histomorphometric method for age-at-death estimation. *Forensic Science International* 296: 48-52

Lanting JN, Aerts-Bijma AT, van der Plicht J, Boaretto E, Carmi I. 2001. Dating of cremated bones. *Radiocarbon* 43: 249-254

Lara M, Paz V, Lewis H, Solheim II W. 2015. Bone modifications in an Early Holocene cremation burial from Palawan, Philippines. *International Journal of Osteoarchaeology* 25: 637-652

Lebon M, Reiche I, Bahain J-J, Chadefaux C, Moigne A-M, Fröhlich F, Sémah F, Schwarcz HP, Falguères C. 2010. New parameters for the characterization of diagenetic alterations and heat-induced changes of fossil bone mineral using Fourier transform infrared spectrometry. *Journal of Archaeological Science* 37: 2265-2276

Lemmers SAM. 2012. Burned culture: osteological research into Urnfield cremation technology and ritual in the South of the Netherlands. *Lunula Archaeologia Protohistorica* 20: 81–88

Lemmers SA, Gonçalves D, Cunha E, Vassalo AR, Appleby J. 2020. Burned fleshed or dry? The potential of bioerosion to determine the pre-burning condition of human remains. *Journal of Archaeological Method and Theory* 27: 972-991

Lisowski FP. 1968. The investigation of human cremations. *Anthropologie und Humangenetik* 4: 76–83

Lowrance EW, Latimer HB. 1957. Weights and linear measurements of 105 skeletons from Asia. *The American Journal of Anatomy* 101: 445–459

Lyman RL. 1994. *Vertebrate taphonomy.* Cambridge: Cambridge University Press

Malinowski A, Porawski R. 1969. Identifikationsmöglichkeiten Menschlicher Brandknochen mit Besonderer Berücksichtigung Ihres Gewichts. *Zacchia* 5: 1–19

Mamede AP, Gonçalves D, Marques MPM, Batista de Carvalho LAE. 2017. Burned bones tell their own stories: A review of methodological approaches to assess heat-induced diagenesis. *Applied Spectroscopy Reviews* 53: 603-635

Marciniak S-M. 2009. A preliminary assessment of the identification of saw marks on burned bone. *Journal of Forensic Sciences* 54: 779-785

Marella GL, Perfetti E, Arcudi G. 2012. Differential diagnosis between cranial fractures of traumatic origin and explosion fractures in burned cadavers. *Journal of Forensic and Legal Medicine* 19: 175-178

Masotti S, Pasini A, Gualdi-Russo E. 2019. Sex determination in cremated human remains using the lateral angle of the pars petrosa ossis temporalis: is old age a limiting factor? *Forensic Science, Medicine and Pathology* 15: 392–398

Masotti S, Mongillo J, Gualdi-Russo E. 2020. Burned human remains: diachronic analysis of cremation rituals in necropolises of northern Italy. *Archaeological and Anthropological Sciences* 12: 74

May SE. 2011. The effects of body mass on cremation weight. *Journal of Forensic Sciences* 56: 3-9

Mayne PM. 1990. *The identification of precremation trauma in cremated bone.* MA thesis, University of Alberta

Mayne Correia PM. 1997. *Fire modification of bone: A review of the literature.* In: Haglund WD, Sord MH (eds.) Forensic taphonomy: The post-mortem fate of human remains. Boca Raton: CRC Press; pp. 275-293

Mayne Correia P, Beattie O. 2002. *A critical look at methods for recovering, evaluating, and interpreting cremated human remains.* In: Haglund WD, Sorg MH (eds.) Advances in forensic taphonomy: Method, theory, and archaeological perspectives. Boca Raton: CRC Press; pp. 435-450

McCutcheon PT. 1992. *Burned archaeological bone.* In: Stein J (ed.) Deciphering a shell midden. San Diego: Academic Press; pp. 347-370

McKinley JI. 1993. Bone fragment size and weights of bone from modern British cremations and the implicat ons for the interpretation of archaeological cremations. *International Journal of Osteoarchaeology* 3: 283-287

McKinley JI. 1994a. *Spong Hill Part VIII: The cremations.* East Dereham, Norfolk: East Anglian Archaeology 69

McKinley JI. 1994b. Bone fragment size in British cremation burials and its implications for pyre technology and ritual. *Journal of Archaeological Science* 21: 339–342

McKinley JI. 2000. *The analysis of cremated bone.* In: Cox M, Mays S (eds.) Human osteology. London: Greenwich Medical Media; pp. 403–421

McKinley JI. 2006. *Cremation...the cheap option?* In: Knusel C, Gowland R (eds.) The social archaeology of funerary remains. Oxford: Oxbow Books; pp. 81–88

McKinley JI. 2015. *In the heat of the pyre.* In: Schmidt CW, Symes SA (eds.) The analysis of burned human remains, 2nd edition. Amsterdam: Elsevier; pp. 181-202

McKinley JI. 2017. *Compiling a skeletal inventory: cremated human bone.* In: Mitchell PD, Brickley M (eds.) Updated guidelines to the standards for recording human remains. Chartered Institute for Archaeologists and British Association for Biological Anthropology and Osteoarchaeology; pp. 14-19

McKinley J, Bond JM. 2001. *Cremated bone.* In: Brothwell D, Pollard A (eds.) Handbook of archaeological sciences. Chichester: John Wiley and Sons; pp. 281-292

Minami M, Mukumoto H, Wakaki S, Nakamura T. 2019. Effect of crystallinity of apatite on cremated bone on carbon exhanges during burial and reliability of radiocarbon dating. *Radiocarbon* 61: 1823-1834

Minozzi S. 2015. *Italian Iron Age cremations.* In: Schmidt CW, Symes SA (eds.) The analysis of burned human remains, 2nd edition. Amsterdam: Elsevier; pp. 307-322

Müller M, Depreux R, Muller P, Fontaine M. 1952. Recherches anthropologiques sur les ossements retrouvés dans des urnes Puniques. *Bulletins et Mémoires de la Société d'Anthropologie de Paris* 3: 160–173

Munro LE, Longstaffe FJ, White CD. 2007. Burning and boiling of modern deer bone: Effects on crystallinity and oxygen isotope composition of bioapatite phosphate. Palaeogeography, Palaeoclimatology, *Palaeoecology* 249: 90–102

Murad TA. 1998. *The growing popularity of cremation versus inhumation: Some forensic implications.* In: Reichs K (ed.) Forensic osteology: Advances in the identification of human remains. Springfield, IL: Charles C. Thomas; pp. 86-105

Murray KA, Rose JC. 1993. The analysis of cremains: A case study involving the inappropriate disposal of mortuary remains. *Journal of Forensic Sciences* 38: 98-103

Nagy G, Lorand T, Patonai Z, Montsko G, Bajnoczky I, Marcsik A, Mark L. 2008. Analysis of pathological and non-pathological human skeletal remains by FT-IR spectroscopy. *Forensic Science International* 175: 55–60

Naji S, de Becdelievre C, Djouad S, Duday H, André A, Rottier S. 2014. *Recovery methods for cremated commingled remains: analysis and interpretation of small fragments using a bioarchaeological approach.* In: Adams BJ, Byrd JE (eds.) Commingled human remains: methods in recovery, analysis, and identification. San Diego: Academic Press; pp. 35-56

Nakano T, Tokumura A, Umakoshi Y. 2002. Variations in crystallinity of hydroxyapatite and the related calcium phosphate by mechanical grinding and subsequent heat treatment. *Metallurgical and Materials Transactions* A 33: 521–528

Naysmith P, Scott EM, Cook GT, Heinemeier J, van der Plicht J, Van Strydonck M, Ramsey CB, Grootes PM, Freeman SPHT. 2007. A cremated bone intercomparison study. *Radiocarbon* 49: 403-408

Nelson R. 1992. A microscopic comparison of fresh and burned bone. *Journal of Forensic Sciences* 37: 1055-1060

Nelson K, Melton T. 2007. Forensic mitochondrial DNA analysis of 116 casework skeletal samples. *Journal of Forensic Sciences* 52: 557-561

Nicholson R. 1993. A morphological investigation of burnt animal bone and an evaluation of its utility in archaeology. *Journal of Archaeological Science* 20: 411–428

Nikita E, Lahr MM. 2011. Simple algorithms for the estimation of the initial number of individuals in commingled skeletal remains. *American Journal of Physical Anthropology* 146: 629-636

Nikita E, Karligkioti A, Lee H. 2019. *Excavation and study of commingled human skeletal remains.* Nicosia: The Cyprus Institute

Olsen J, Heinemeier J, Bennike P, Krause C, Hornstrup KM, Thrane H. 2008. Characterisation and blind testing of radiocarbon dating of cremated bone. *Journal of Archaeological Science* 35: 791–800

Olsen J, Hornstrup KM, Heinemeier J, Bennike P, Thrane H. 2011. Chronology of the Danish Bronze Age based on 14C dating of cremated bone remains. *Radiocarbon* 53: 261–275

Olsen J, Heinemeier J, Hornstrup KM, Bennike P, Thrane H. 2013. 'Old wood' effect in radiocarbon dating of prehistoric cremated bones? *Journal of Archaeological Science* 40: 30-34

Paine RR, Brenton BP. 2006. Dietary health does affect histological age assessment: an evaluation of the Stout and Paine (1992) age estimation equation using secondary osteons from the rib. *Journal of Forensic Sciences* 51: 489-492

Paschalis EP, Betts F, DiCarlo E, Mendelsohn R, Boskey AL. 1997. FTIR microspectroscopic analysis of normal human cortical and trabecular bone. *Calcified Tissue International* 61: 480-486

Person A, Bocherens H, Mariotti A, Renard M. 1996. Diagenetic evolution and experimental heating of bone phosphate. *Palaeogeography, Palaeoclimatology, Palaeoecology* 126: 135–149

Petersohn F, Köhler J. 1965. Die bedeutung der veräderungen an fetalen röhrenknochen nach trocknung und hitzeeinwirkung für die forensische begutachtung der fruchgrösse. *Archive für Kriminologie* 134: 143

Piga G, Thompson TJU, Malgosa A, Enzo S. 2009. The potential of X-Ray diffraction in the analysis of burned remains from forensic contexts. *Journal of Forensic Sciences* 54: 534-539

Pijoan CMA, Mansilla J, Leboreiro I, Lara VH, Bosch P. 2007. Thermal alterations in archaeological bones. *Archaeometry* 49: 713–727

Piontek J. 1975. Polish method and results of investigations of cremated bones from prehistoric cemeteries. *Glasnik Anthropoloskog Drustva Jugoslavise Sveska* 12: 23–34

Pope E. 2007. Burned human remains: myths in forensic sciences. *Proceedings of the American Academy of Forensic Sciences* 13: 379–380

Pope EJ, Smith C. 2004. Identification of traumatic injury in burned cranial bone: an experimental approach. *Journal of Forensic Sciences* 49: 431-440

Pucéat E, Reynard B, Lécuyer C. 2004. Can crystallinity be used to determine the degree of chemical alteration of biogenic apatites? *Chemical Geology* 205: 83-97

Pusch CM, Broghammer M, Scholz M. 2000. Cremation practices and the survival of ancient DNA: burnt bone analyses via RAPD-mediated PCR. *Anthropologischer Anzeiger* 58: 237–251

Rees KA, Cox MJ. 2010. Comparative analysis of the effects of heat on the PCR amplification of various sized DNA fragments extracted from sus scrofa molars. *Journal of Forensic Sciences* 55: 410-417

Reinhard KJ. 1994. Cremation in Southwestern North America: aspects of taphonomy that affect pathological analysis. *Journal of Archaeological Science* 21: 597-605

Rhine S. 1998. *Bone voyage: a journey in forensic anthropology.* Albuquerque: University of New Mexico Press

Richier A. 2005. *Sépultures primaires à incineration: Nouvelles données et nouvelles problématiques.* In: Mordant C, Depierre G (eds.) Les pratiques funéraires à l'Âge du Bronze en France. Paris: Comité des Travaux Historiques et Scientifiques; pp. 199-210

Robbins SC, Fairgrieve SI, Oost TS. 2015. Interpreting the effects of burning on pre-incineration saw marks in bone. *Journal of Forensic Sciences* 60: S182-S187

Robinson JR, Kingston JD. 2020. Burned by the fire: Isotopic effects of experimental combustion of faunal tooth enamel. *Journal of Archaeological Science: Reports* 34: 102593

Rogers KD, Daniels P. 2002. An X-ray diffraction study of the effects of heat treatment on bone mineral microstructure. *Biomaterials* 23: 2577–2585

Rogers K, Beckett S, Kuhn S, Chamberlain A, Clement J. 2010. Contrasting the crystallinity indicators of heated and diagenetically altered bone mineral. *Palaeogeography, Palaeoclimatology, Palaeoecology* 296: 125–129

Rose HA, Meadows J, Henriksen MB. 2020. Bayesian modelling of wood-age offsets in cremated bone. *Radiocarbon* 62: 379-401

Rosen F. 2004. *Cremation in America.* New York: Prometheus Books

Rösing FW. 1977. Methoden und Aussagemöglichkeiten der Anthropologischen Leichengrandbearbeitung. *Archaeologie und Naturwissenschaften* 1: 53–80

Rubini M, Licitra M, Baleani M. 1997. A study of cremated human remains from an urn field dating to the final phase of the Bronze Age, found at "Le Caprine" (Guidonia, Rome, Italy 10th-9th century B.C.) *International Journal of Anthropology* 12: 1-9

Sajantila A, Ström M, Budowle B, Karhunen PJ, Peltonen L. 1991. The polymerase chain reaction and post-mortem forensic identity testing: application of amplified D1S80 and HLA-DQa loci to the identification of fire victims. *Forensic Science International* 51: 23–34

Sakoda S, Zhu BL, Ishida K, Oritani S, Fujita MQ, Maeda H. 2000. Dental identification in routine forensic casework: clinical and postmortem investigations. *Legal Medicine* 2: 7–14

Sandholzer M. 2015. *Influence of heating regimes on dimensional and colorimetric changes of teeth.* In: Schmidt CW, Symes SA (eds.) The analysis of burned human remains, 2nd edition. Amsterdam: Elsevier; pp. 365-379

Sandholzer MA, Walmsley AD, Lumley PJ, Landini G. 2013. Radiologic evaluation of heat-induced shrinkage and shape preservation of human teeth using micro-CT. *Journal of Forensic Radiology and Imaging* 1: 107–111

Sandholzer MA, Baron K, Heimel P, Metscher BD. 2014a. Volume analysis of heat-induced cracks in human molars: A preliminary study. *Journal of Forensic Dental Sciences* 6: 139-144

Sandholzer MA, Sui T, Korsunsky AM, Walmsley AD, Lumley PJ, Landini G. 2014b. X-ray scattering evaluation of ultrastructural changes in human dental tissues with thermal treatment. *Journal of Forensic Sciences* 59: 769-774

Schmidt CW. 2015. *Burned human teeth.* In: Schmidt CW, Symes SA (eds.) The analysis of burned human remains, 2nd edition. Amsterdam: Elsevier; pp. 61-81

Schmidt CW, Symes SA. 2015. *The analysis of burned human remains, 2nd edition.* Amsterdam: Elsevier

Schmidt CW, Tomak C, Lockhart RA, Greene TR, Reinhardt GA. 2015. *Early Archaic cremations from Southern Indiana.* In: Schmidt CW, Symes SA (eds.) The analysis of burned human remains, 2nd edition. Amsterdam: Elsevier; pp. 247-258

Schultz JJ, Warren MW, Krigbaum JS. 2015. *Analysis of human cremains.* In: Schmidt CW, Symes SA (eds.) The analysis of burned human remains, 2nd edition. Amsterdam: Elsevier; pp. 83-103

Schurr MR, Hayes RG, Cook DC. 2015. *Thermally induced changes.* In: Schmidt CW, Symes SA (eds.) The analysis of burned human remains, 2nd edition. Amsterdam: Elsevier; pp. 105-118

Schutkowski H. 1983. Über den diagnostischen Wert der Pars petrosa ossis temporalis für die Geschlechtsbestimmung. *Zeitschrift für Morphologie und Anthropologie* 74: 129-144

Schutkowski H, Herrmann B. 1983. Zur MÖglichkeit der metrischen geschlechtsdiagnose an der Pars petrosa ossis temporalis. *Zeitschrift für Rechtsmedizin* 90: 219-227

Schwark T, Heinrich A, Preuße-Prange A, von Wurmb-Schwark N. 2011. Reliable genetic identification of burnt human remains. *Forensic Science International Genetics* 5: 393-399

Shipman P, Foster G, Schoeninger M. 1984. Burnt bones and teeth: an experimental study of color, morphology, crystal structure and shrinkage. *Journal of Archaeological Science* 11: 301-325

Silva AM, Crubézy E, Cunha E. 2009. Bone weight: new reference values based on a modern Portuguese identified skeletal collection. *International Journal of Osteoarchaeology* 19: 628–641

Smits E. 1998. Étude anthropologique des restes incinérés de la nécropole laténienne d'ursel (flandre orientale, belgique). *Revue Archéologique de Picardie* 1-2: 127-134

Snoeck C, Brock F, Schulting RJ. 2014. Carbon exchanges between bone apatite and fuels during cremation: impact on radiocarbon dates. *Radiocarbon* 56: 591–602

Snoeck C, Lee-Thorp J, Schulting R, de Jong J, Debouge W, Mattielli N. 2015. Calcined bone provides a reliable substrate for strontium isotope ratios as shown by an enrichment experiment. *Rapid Communications in Mass Spectrometry* 29: 107–114

Snoeck C, Pouncett J, Ramsey G, Meighan IG, Mattielli N, Goderis S, Lee-Thorp JA, Schulting RJ. 2016. Mobility during the Neolithic and Bronze Age in Northern Ireland explored using strontium isotope analysis of cremated human bone. *American Journal of Physical Anthropology* 160: 397-413

Snoeck C, Pouncett J, Claeys P, Goderis S, Mattielli N, Pearson MP, Willis C, Zazzo A, Lee-Thorp JA, Schulting RJ. 2018. Strontium isotope analysis on cremated human remains from Stonehenge support links with west Wales. *Scientific Reports* 8: 10790

Spennemann DHR, Colley SM. 1989. Fire in a pit: the effects of burning on faunal remains. *Archaeozoologia* 3: 51–64

Spitz WU. 1993. *Thermal injuries.* In: Spitz WU (ed.) Spitz and Fisher's medicolegal investigation of death, 3rd edition. Springfield, IL: Charles C. Thomas; pp. 413-443

Stewart TD. 1979. *Essentials of forensic anthropology.* Springfield, IL: Charles C. Thomas

Stiner MC, Kuhn SL, Weiner S, Bar-Yosef O. 1995. Differential burning, recrystallization, and fragmentation of archaeological bone. *Journal of Archaeological Science* 22: 223–237

Stiner MC, Kuhn SL, Surovell TA, Goldberg P, Meignen L, Weiner S, Bar-Yosef O. 2001. Bone preservation in Hayonim Cave (Israel): a macroscopic and mineralogical study. *Journal of Archaeological Science* 28: 643–659

Sui T, Sandholzer MA, Lunt AJG, Baimpas N, Smith A, Landini G, Korsunsky AM. 2014. In situ X-ray scattering evaluation of heat-induced ultrastructural changes in dental tissues and synthetic hydroxyapatite. *Journal of the Royal Society Interface* 11: 20130928

Surovell TA, Stiner MC. 2001. Standardizing infra-red measures of bone mineral crystallinity: an experimental approach. *Journal of Archaeological Science* 28: 633–642

Symes SA, Dirkmaat DC, Ousley S, Chapman E, Cabo L. 2012. *Recovery and interpretation of burned human remains.* Final Technical Report Award 2008-DN-BX-K131

Symes SA, L'Abbé EN, Pokines JT, Yuzwa T, Messer D, Stromquist A, Keough N. 2013. *Thermal alteration to bone.* In: Pokines JT, Symes SA (eds.) Manual of forensic taphonomy. Boca Raton: CRC Press; pp. 367-402

Symes SA, Rainwater CW, Chapman EN, Gipson DR, Piper AL. 2015. *Patterned thermal destruction in a forensic setting.* In: Schmidt CW, Symes SA (eds.) The analysis of burned human remains, 2nd edition. Amsterdam: Elsevier; pp. 17-59

Taylor N, Frei KM, Frei R. 2020. A strontium isotope pilot study using cremated teeth from the Vollmarshausen cemetery, Hesse, Germany. *Journal of Archaeological Science: Reports* 31: 102356

Thompson TJU. 2003. *An experimental study of the effects of heating and burning on the hard tissues of the human body, and its implications for anthropology and forensic science.* PhD thesis, University of Sheffield

Thompson TJU. 2004. Recent advances in the study of burned bone and their implications for forensic anthropology. *Forensic Science International* 146: S203–S205

Thompson TJU. 2005. Heat-induced dimensional changes in bone and their consequences for forensic anthropology. *Journal of Forensic Sciences* 50: 1008-1015

Thompson TJU. 2015. *Fire and the body: Fire and the people.* In: Thompson TJU (ed.) The archaeology of cremation. Burned human remains in funerary studies. Oxford: Oxbow Books; pp. 1-17

Thompson TJU, Gauthier M, Islam M. 2009. The application of a new method of Fourier Transform Infrared Spectroscopy to the analysis of burned bone. *Journal of Archaeological Science* 36: 910-914

Thompson TJU, Islam M, Piduru K, Marcel A. 2011. An investigation into the internal and external variables acting on crystallinity index using Fourier Transform Infrared Spectroscopy on unaltered and burned bone. *Palaeogeography, Palaeoclimatology, Palaeoecology* 299: 168–174

Thompson TJU, Gonçalves D, Squires K, Ulguim P. 2017. *Thermal alteration to the body.* In: Schotsmans EMJ, Márquez-Grant N, Forbes SL (eds.) Taphonomy of human remains: Forensic analysis of the dead and the depositional environment. New York: John Wiley & Sons; pp. 318-334

Thurman M, Willmore L. 1980. A replicative cremation experiment. *North American Archaeologist* 2: 275–283

Trotter M, Peterson RR. 1962. The relationship of ash weight and organic weight of human skeletons. *Journal of Bone and Joint Surgery* 44: 669–681

Trueman CN, Privat K, Field J. 2008. Why do crystallinity values fail to predict the extent of diagenetic alteration of bone mineral? *Palaeogeography, Palaeoclimatology, Palaeoecology* 266: 160–167

Tsuchimochi T, Iwasa M, Maeno Y, Koyama H, Inoue H, Isobe I, Matoba R, Yokoi M, Nagao M. 2002. Chelating resin-based extraction of DNA from dental pulp and sex determination from incinerated teeth with Y-chromosomal alphoid repeat and short tandem repeats. *American Journal of Forensic Medicine and Pathology* 23: 268–271

Tutor PM, Márquez-Grant N, Rojas CV, García AM, Guzmán IP, Sánchez MB. 2020. Through fire and flames: post-burning survival and detection of dismemberment-related toolmarks in cremated cadavers. *International Journal of Legal Medicine* https://doi.org/10.1007/s00414-020-02447-1

Tutor PM, Sánchez MB, Rojas CV, García AM, Guzmán IP, Márquez-Grant N. 2021. Cut or burnt? – Categorizing morphological characteristics of heat-induced fractures and sharp force trauma. *Legal Medicine* 50: 101868

Ubelaker DH. 2009. The forensic evaluation of burned skeletal remains: A synthesis. *Forensic Science International* 183: 1-5

Ulguim PF. 2015. *Analysing cremated human remains from the southern Brazilian highlands: Interpreting archaeological evidence of funerary practice at mound and enclosure complexes in the Pelotas River Valley.* In: Thompson TJU (ed.) The archaeology of cremation: burned human remains in funerary studies. Oxford: Oxbow Press; pp. 173-212

Van Deest TL, Murad TA, Bartelink EJ. 2011. A re-examination of cremains weight: sex and age variation in a Northern California sample. *Journal of Forensic Sciences* 56: 344-349

Van Strydonck M, Boudin M, Hoefkens M, De Mulder G. 2005. 14C-dating of cremated bones, why does it work? Lunula. *Archaeologia Protohistorica* 13: 3-10

Van Strydonck M, Boudin M, De Mulder G. 2009. 14C dating of cremated bones: the issue of sample contamination. *Radiocarbon* 51: 553-568

Van Strydonck M, Boudin M, De Mulder G. 2010. The carbon origin of structural carbonate in bone apatite of cremated bones. *Radiocarbon* 52: 578-586

Van Vark GN. 1970. *Some statistical procedures for the investigation of prehistoric skeletal material.* Master's thesis, University of Gröningen

Van Vark GN. 1974. The investigation of human cremated skeletal material by multivariate statistical methods I. Methodology. *Ossa* 1: 63-95

Van Vark GN. 1975. The investigation of human cremated skeletal material by multivariate statistical methods II. Measures. *Ossa* 2: 47-68

Van Vark GN, Amesz-Voorhoeve W, Cuijpers A. 1996. Sex-diagnosis of human cremated skeletal material by means of mathematical-statistical and data-analytical methods. *Homo* 47: 305-338

Végh EI, Czermak A, Márquez-Grant N, Schulting RJ. 2021. Assessing the reliability of microbial bioerosion features in burnt bones: A novel approach using feature-labelling in histotaphonomical analysis. *Journal of Archaeological Science: Reports* 37: 102906

Wahl J. 2015. *Investigations on pre-Roman and Roman cremation remains.* In: Schmidt CW, Symes SA (eds.) The analysis of burned human remains, 2nd edition. Amsterdam: Elsevier; pp. 163-179

Walker PL, Miller KWP, Richman R. 2008. *Time, temperature, and oxygen availability: An experimental study of the effects of environmental conditions on the color and organic content of cremated bone.* In: Schmidt CW, Symes SA (eds.) The analysis of burned human remains. Amsterdam: Elsevier; pp. 129-135

Waltenberger L, Schutkowski H. 2017. Effects of heat on cut mark characteristics. *Forensic Science International* 271: 49-58

Wärmländer SKTS, Varul L, Koskinen J, Saage R, Schlager S. 2019. Estimating the temperature of heat-exposed bone via machine learning analysis of SCI color values: a pilot study. *Journal of Forensic Sciences* 64: 190-195

Warren MW, Maples WR. 1997. The anthropometry of contemporary commercial cremation. *Journal of Forensic Sciences* 42: 417-423

Watson JT, Cerezo-Román JI, Maldonado SIN, Guzmán CC, Villalpando ME. 2015. *Death and community identity in the Trincheras cremation cemetery, Sonora, Mexico.* In: Schmidt CW, Symes SA (eds.) The analysis of burned human remains, 2nd edition. Amsterdam: Elsevier; pp. 339-353

Weitzel MA, McKenzie HG. 2015. *Fire as a cultural taphonomic agent.* In: Schmidt CW, Symes SA (eds.) The analysis of burned human remains, 2nd edition. Amsterdam: Elsevier; pp. 203-217

Whyte TR. 2001. Distinguishing remains of human cremations from burned animal bones. *Journal of Field Archaeology* 28: 437-448

Williams D, Lewis M, Franzen T, Lissett V, Adams C, Whittaker D, Tysoe C, Butler R. 2004. Sex determination by PCR analysis of DNA extracted from incinerated, deciduous teeth. *Science and Justice* 44: 89-94

Wright LE, Schwarcz HP. 1996. Infrared and isotopic evidence for diagenesis of bone apatite at Dos Pilas, Guatemala: palaeodietary implications. *Journal of Archaeological Science* 23: 933–944

von Wurmb-Schwark N, Simeoni E, Ringleb A, Oehmichen M. 2004. Genetic investigation of modern burned corpses. *International Congress Series* 1261: 50-52

Zana M, Magli F, Mazzucchi A, Castoldi E, Gibelli D, Caccia G, Cornacchia F, Gaudio DA, Mattia M, Cattaneo C. 2017. Effects of cremation on fetal bones. *Journal of Forensic Sciences* 62: 1140-1144

Zazzo A, Saliège JF, Lebon M, Lepetz S, Moreau C. 2012. Radiocarbon dating of calcined bones: insights from combustion experiments under natural conditions. *Radiocarbon* 54: 855-866

RECORDING SHEETS

RECORDING SHEET FOR BURNED HUMAN SKELETAL REMAINS

This recording sheet largely draws from that proposed for commingled remains (STARC Guide No. 2)

The forms given here are for individual unassociated skeletal elements, which is the most common state in which burned remains are retrieved. Note that when working with such remains, it is generally impractical to use printed forms. Instead, try to fit the information given below in a spreadsheet (e.g. in Excel) whereby each individual element occupies a row and each variable is given in a column.

GENERAL INFORMATION	
Archaeological site:	
Curation site:	
Recorder:	
Date:	
Burial No:	
Grave type:	
Grave size:	
Field methods for site identification:	
Field methods for site excavation:	
Cleaning methods:	
Restoration methods:	

BONE INVENTORY

Key: Zones as defined by Knüsel and Outram (2004); record expression per zone as 0 = absent, 1 = present <25%, 2 = present 26-50%, 3 = present 51-75%, 4 = present >76% or simply as 0 = absent, 1 = present

CRANIUM, MANDIBLE, EAR OSSICLES & HYOID

Element	Zone/Side	Expression	Element	Zone/Side	Expression
Frontal	1		Vomer	–	
	2		Lacrimal		
Parietal	3		Palatine		
	4		Ethmoid	–	
Occipital	5		Mandible	1	
Temporal	6			2	
	7			3	
Sphenoid	8			4	
	9			5	
Zygomatic	10			6	
	11			7	
Maxilla	12		Malleus		
	13		Stapes		
Nasal	14		Incus		
	15		Hyoid	–	
Inferior nasal concha					

THORACIC CAGE & VERTEBRAE

Element	Zone	Left	Right	Element	Zone	Expression
Sternum	1			Atlas	1	
	2				2	
	3				3	
Rib 1	1				4	
	2			Axis	1	
	3				2	
Rib 2	1				3	
	2				4	
	3			C3-7	1	
Rib 3-10	1				2	
	2				3	
	3				4	
Rib 11	1			T1-12	1	
	2				2	
	3				3	
Rib 12	1				4	
	2			L1-5	1	
	3				2	
					3	
					4	

SHOULDER GIRDLE

Element	Zone	Left	Right	Element	Zone	Left	Right
Clavicle	1			Scapula	1		
	2				2		
	3				3		
					4		
					5		
					6		
					7		
					8		
					9		

UPPER AND LOWER LIMB LONG BONES & PATELLA							
Element	Zone	Left	Right	Element	Zone	Left	Right
Humerus	1			Femur	1		
	2				2		
	3				3		
	4				4		
	5				5		
	6				6		
	7				7		
	8				8		
	9				9		
	10				10		
	11				11		
Radius	1			Patella	–		
	2			Tibia	1		
	3				2		
	4				3		
	5				4		
	6				5		
	7				6		
	8				7		
	9				8		
	10				9		
	11				10		
	J			Fibula	1		
Ulna	A & B				2		
	C				3		
	D				4		
	E				5		
	F				6		
	G						
	H						
	J						

HAND BONES									
Element	Zone	Left	Right		Element	Zone	Left	Right
Scaphoid	–				MC4	1		
Lunate	–					2		
Triquetral	–					3		
Pisiform	–				MC5	1		
Trapezium	–					2		
Trapezoid	–					3		
Capitate	–				Proximal phalanx	1		
Hamate	–					2		
MC1	1					3		
	2				Middle phalanx	1		
	3					2		
MC2	1					3		
	2				Distal phalanx	1		
	3					2		
MC3	1					3		
	2							
	3							

PELVIC BONES									
Element	Zone	Left	Right		Element	Zone	Left	Right
Os coxa	1				Sacrum	1		
	2					2		
	3					3		
	4					4		
	5							
	6							
	7							
	8							
	9							
	10							
	11							
	12							

FOOT BONES							
Element	Zone	Left	Right	Element	Zone	Left	Right
Talus	1			MT3	1		
	2				2		
	3				3		
	4			MT4	1		
Calcaneus	1				2		
	2				3		
	3			MT5	1		
	4				2		
	5				3		
Navicular	–			Proximal phalanx	1		
Cuboid	–				2		
1st Cuneiform	–				3		
2nd Cuneiform	–			Middle phalanx	1		
3rd Cuneiform	–				2		
MT1	1				3		
	2			Distal phalanx	1		
	3				2		
MT2	1				3		
	2						
	3						

BROADLY IDENTIFIED BONE							
Type	Size class	No of fragments	Weight	Type	Size class	No of fragments	Weight
Cranium	<1 cm			Pelvic girdle	<1 cm		
	1-3 cm				1-3 cm		
	3-5 cm				3-5 cm		
	>5cm				>5cm		
Thorax	<1 cm			Lower limb	<1 cm		
	1-3 cm				1-3 cm		
	3-5 cm				3-5 cm		
	>5cm				>5cm		
Pectoral girdle	<1 cm			Unidentifiable	<1 cm		
	1-3 cm				1-3 cm		
	3-5 cm				3-5 cm		
	>5cm				>5cm		
Upper limb	<1 cm						
	1-3 cm						
	3-5 cm						
	>5cm						

UNIDENTIFIED BONE							
Type	Size class	No of fragments	Weight	Type	Size class	No of fragments	Weight
Flat	<1 cm			Long - epiphysis	<1 cm		
	1-3 cm				1-3 cm		
	3-5 cm				3-5 cm		
	>5cm				>5cm		
Short	<1 cm			Long - diaphysis	<1 cm		
	1-3 cm				1-3 cm		
	3-5 cm				3-5 cm		
	>5cm				>5cm		

DENTAL INVENTORY

Key: 1 = Present, not in occlusion, 2 = Present, development completed, in occlusion, 3 = Missing, no associated alveolar bone, 4 = Missing, antemortem loss, 5 = Missing, postmortem loss, 6 = Missing, congenital absence, 7 = Present, damage renders measurement impossible, 8 = Present, unobservable

PERMANENT TEETH		I1	I2	C	P3	P4	M1	M2	M3
Maxilla	Left								
Maxilla	Right								
Mandible	Left								
Mandible	Right								

DECIDUOUS TEETH		I1	I2	C	M1	M2
Maxilla	Left					
Maxilla	Right					
Mandible	Left					
Mandible	Right					

HEAT-INDUCED ALTERATION

Skeletal/ dental fragment	Preservation of organics[1]	Fracturing[2]	Shrinkage[3]	Warping[4]	Discoloration[5]	Pre-incineration state[6]	Crystallinity index

[1] Record as 'carbonization' or 'calcination'

[2] Record as longitudinal, step, transverse, patina, splintering and delamination, burn line, and curved transverse

[3] Record only when clearly visible (e.g. when bilateral asymmetry is noted in elements diferentially exposed to heat); otherwise leave blank

[4] Record as present/absent

[5] Record using Munsell Soil Color Chart or any other available method (e.g. RGB)

[6] Record as dry or fleshed; assessed via warping, fracturing, and discoloration

SEX ASSESSMENT (ONLY FOR ADULT REMAINS)

Key: Record as Female, Probable Female, Ambiguous, Probable Male, Male, Indeterminate

Element	Trait/Method	Sex

AGE-AT-DEATH ESTIMATION (FOR NONADULTS)

Classify individuals in one of the following categories: fetus = before birth, infant = 0-3 yrs, child = 3-12 yrs, adolescent = 12-20 yrs, nonadult = <18 yrs, indeterminate = unable to estimate age-at-death

Element	Trait/Method	Age-at-death

AGE-AT-DEATH ESTIMATION (FOR ADULTS)

Classify individuals in one of the following categories: young adult = 20-35 yrs, middle adult = 35-50 yrs, old adult = 50+ yrs, adult = 18+ yrs, indeterminate = unable to estimate age-at-death

Element	Method	Stage	Age-at-death

PATHOLOGICAL LESIONS

Element affected	Type of lesion	Degree of expression

PROMISE

RESEARCH
& INNOVATION
FOUNDATION

Structural Funds
of the European Union in Cyprus